NATIONAL AND KAPODISTRIAN UNIVERSITY OF ATHENS

Faculty of Geology and Geoenvironment

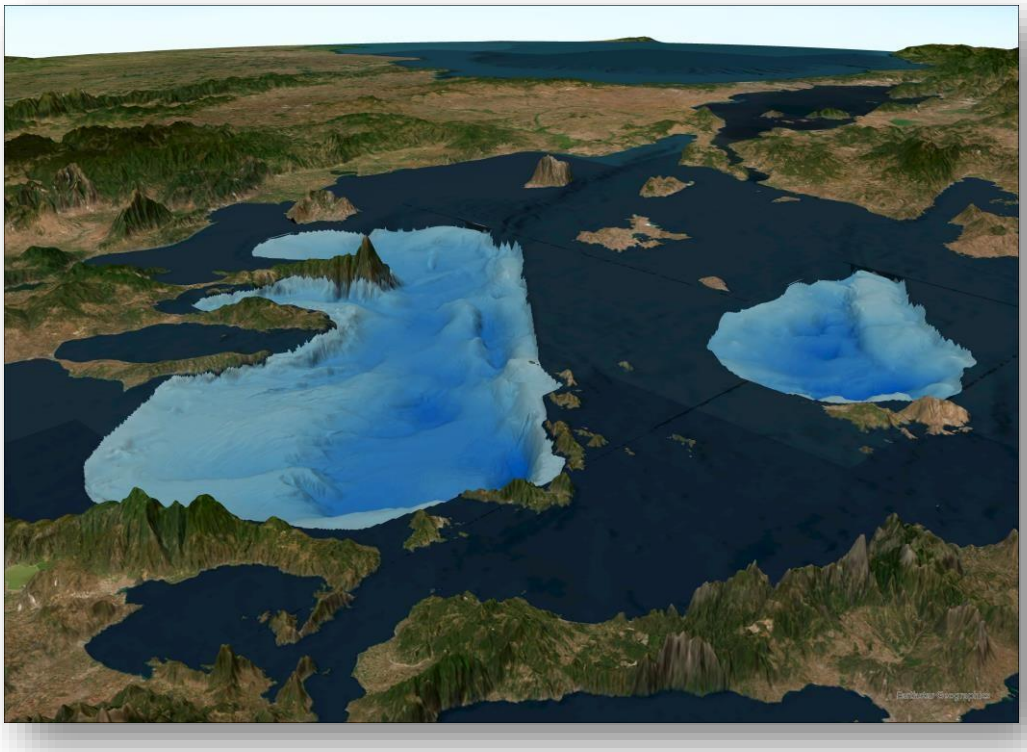

"Morphotectonic Analysis of the North Aegean and Skyros Basins"

BSc Thesis

Author: Stylianos Tampourakis

Supervisor: Dr. Paraskevi V. Nomikou

Athens 2023

CONTENTS

TABLE OF FIGURES

ACKNOWLEDGEMENTS

Firstly, I would like to express my sincere gratitude to my thesis supervisor Assistant Prof. Paraskevi V. Nomikou, of the Sector of Geography & Climatology, Faculty of Geology and Geoenvironment, National and Kapodistrian University of Athens, for her continuous support, her patience, her motivation, and immense knowledge. She inspired me and introduced me to the scientific field of Marine Geology, helping me push my limits.

Furthermore, I would like to thank my family; my parents, and my brother and sister for supporting me and motivating me throughout writing this thesis and my life in general.

Last but not least, I should express my very profound gratitude to my friends for believing in me, making me feel confident, and motivating me by being diligent themselves.

ABSTRACT

The current thesis focuses on studying the North Aegean Basin and Skyros Basin using bathymetric data and its derivatives. The goal is to analyze the morphotectonic features based on morphological criteria and to track fault lines in the submarine area of the aforementioned basins. A Digital Terrain Model (DTM) of 105x105 meters resolution was used (by the European Marine Observation and Data Network) in ArcGIS. The derivatives of this DTM are; Slope, Shaded Relief, 3D Models, Contours, and the Synthetic Map.

The North Aegean and Skyros Basins are the Western branches of the North Anatolian Fault and are tectonically active areas. The Skyros Basin has a similar structure to the neighboring North Aegean Basin but has smaller dimensions and lower deformation rates which is documented by the shallower depths and the smaller width. Both basins are characterized by NE-SW trending segmented faults that constitute the North Anatolian Fault in the eastern part, and NE-SW faults that dominate the western part and consist of marginal faults.

The morphotectonic analysis shows that these fault segments are active since their location coincides with the areas that present abrupt changes in slope. Consequently, its an area prone to seismic events that in their turn can trigger geological phenomena like submarine landslides with a tsunamigenic potential that could result in catastrophic events.

1. INTRODUCTION

The North Aegean Sea is characterized by a particularly unique morphology on land and sea. This particular morphology is because the area is located on the borders of the Eurasian plate, bordering to the south with the African plate and to the east with the Anatolian Plate. One of the most dominant tectonic structures in the North Aegean Sea is the North Anatolian Fault (NAF). NAF is a strike-slip fault that prolongated into the Aegean Sea in the Early Pliocene or Pleistocene, due to the westward movement of the Anatolian plate. The combination of the extensional regime that was applied on the Aegean due to slab rollback and gravitational spreading, with the strike-slip movement led to the dominance of a transtensional tectonic regime and the formation of the North Aegean Basin (NAB) and possibly the Skyros Basin (SB). However, NAF is not a linear tectonic structure but consists of a series of strike-slip fault segments, and their existence reflects on the complex submarine morphology, which includes many morphological discontinuities.

Those fault segments have a long length and are mostly submarine, but these are responsible for many seismicity events in the North Aegean area. Seismicity events can trigger geological phenomena, like landslides and tsunamis that cause widespread damage and even threaten human lives. To minimize the impact of those catastrophic events is of crucial importance to map these faults, identify the most susceptible areas and understand the morphology of the seafloor in detail.

The aim of the present thesis is the identification and mapping of the morphological and morphotectonic features of the North Anatolian Fault Zone, to study their deformational pattern. To accomplish the previous, a detailed analysis of the submarine morphology was made along the areas of the North Aegean Basin and Skyros Basin, which is documented in chapters 4-5. Lastly, this analysis was made in ArcGIS and is based on the bathymetric data provided by the European Marine Observation and Data Network with a resolution of 105x105 meters.

2. NORTH AEGEAN SEA

2.1. GEODYNAMIC SETTING OF THE NORTH AEGEAN SEA

The Aegean Sea is one of the most active tectonic regions in the eastern Mediterranean Sea (Papanikolaou, Alexandri, Nomikou, & Ballas, 2002), (Figure 1). The North Aegean Basin (NAB) is located in the northern part of the Aegean Sea behind the Hellenic Orogenic Arc, which resulted from the convergence between the African and the Eurasian plates. The Hellenic orogenic arc is running from the Ionian Sea to the W and SW of the Hellenic peninsula to the Libyan and Levantine seas to the S and SE (Le Pichon & Angelier, 1979). This convergence between the two plates is passing to its final stage before collision (Finetti, Papanikolaou, Del Ben, & Karvelis, 1991).

The neotectonic history of the Aegean region can be described as a succession of two different, oblique plate movements in the middle Miocene, that were driven by different regional strain stages, back-arc extension, and westward extrusion of the Anatolian block (Dewey & Şengör, 1979). Aegean back-arc extension was driven by slab rollback from the Middle Eocene (45 Ma) to the Middle Miocene (around 13 Ma), with a velocity of trench retreat of almost 10 $mm \cdot y^{-1}$ (Brun & Sokoutis, 2010) after the closure of the oceanic domains of Vardar and Pindos. That oceanic closure led to the stacking of three continental blocks that are from top to base: Rhodopia, Pelagonia, and Adria (Philippon, Brun, Gueydan, & Sokoutis, 2014). The extension was dominantly accommodated by the coeval exhumation of High-Pressure and High-Temperature metamorphic rocks in the wider area of the Aegean (Lister, Banga, & Feenstra, 1984).

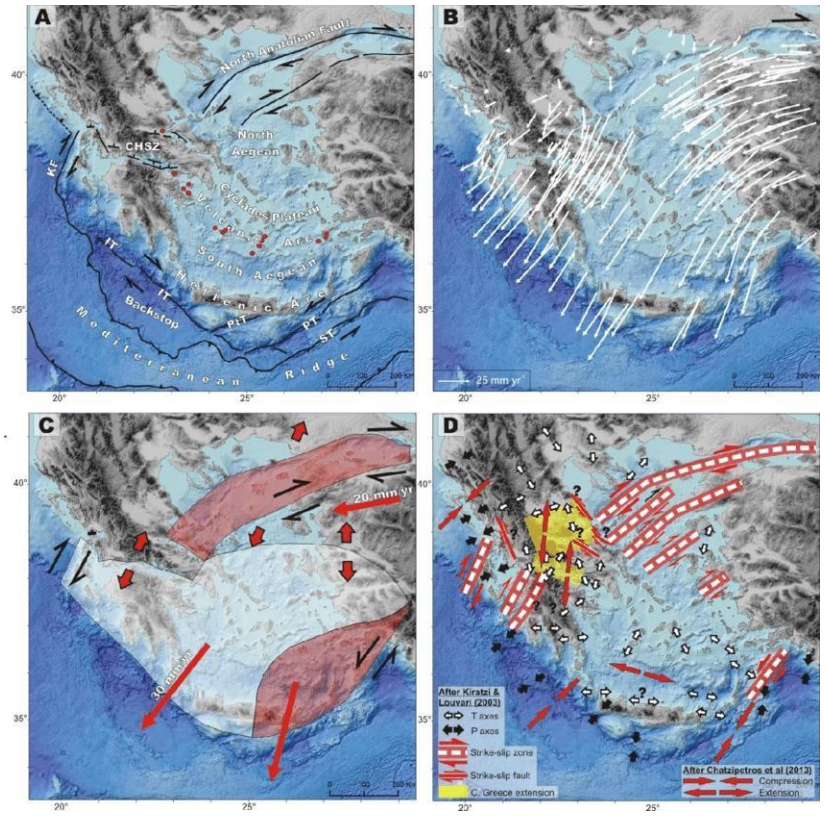

Figure 1. *Major geodynamic elements of the broader Aegean Region, modified after Sakellariou and Tsampouraki-Kraounaki (Dimitriadis, I.; et al. 2009). The white parallelogram delineates the study area. Red dots represent the volcanoes on the Hellenic Volcanic Arc. NAF: North Anatolian Fault, KF: Kephallinia Fault, IT: Ionian Trench, PSF: Pliny-Strabo Trenches, CHRZ: Central Hellenic Relay Zone, SASZ: Santorini-Amorgos Shear Zone. Basins: Cr: Christiana, He: Heraklion, Ka: Karpathos, Kn: Kamilonissi, Ma: Maleas, My: Myrtoon.*

From the Middle Miocene until the present day, the velocity of trench retreat accelerated to almost 33 mm·y^{-1} in the southern Hellenic arc (McClusky, et al., 2000). Due to the acceleration of the extensional rate from 10 to 33 mm·yr^{-1}, the overall Aegean region was fragmented by normal and strike-slip faults, forming extensional basins (Mascle & Martin, 1990), (Figure 2) on the metamorphic domains that were previously exhumed (Philippon, Brun, Gueydan, & Sokoutis, 2014).

In the eastern border of the Mediterranean, the former Tethys Ocean closed in Late Miocene (11–13 Ma ago) and as an aftereffect, the Arabian and the Eurasian plates reached the collisional stage, and consequently, the Anatolian continental block started its lateral westward escape (McKenzie, 1970; Dewey & Şengör, 1979; Le Pichon & Angelier, 1979). The dextral strike-slip shear initiated along the Bitlis Suture led to the formation of the North Anatolian Shear Zone

(NASZ). NASZ at its western end is a 100 kilometers wide wedged–shape zone where the North Anatolian Fault (NAF) formed due to progressive strain localization (Şengör, et al., 2005).

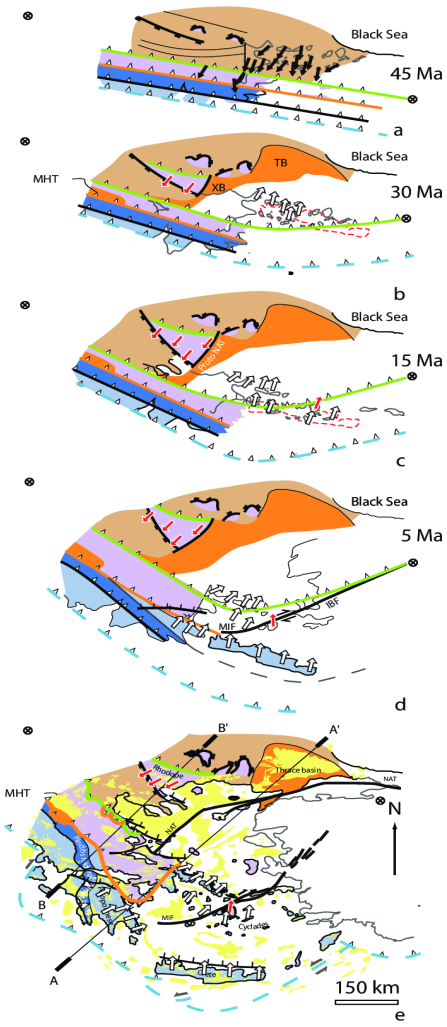

Figure 2. *Map view restoration illustrates the neotectonic extensional history of the Aegean (modified after Brun and Sokoutis (2010)). Time exhumation of HP and HT metamorphic rocks is shown by the blue and green boxes. The yellow box corresponds to the timing of the distributed brittle deformation in the wider Aegean region (Philippon et al., 2014).*

The NAF system propagated westward toward the Aegean domain in the Early Pliocene (about 5 Ma ago) from ties of a vintage seismic dataset with industrial wells, where it is divided into two main strike-slip systems (Figure 3), reaching a bulk offset of 85 kilometers (Armijo, Meyer, Hubert, & Barka, 1999; Hubert-Ferrari, et al., 2003; Şengör, et al., 2005; Beniest, et al., 2016). The northern, main fault segment runs along the Saros Gulf (Kurt, Demirbağ, & Kuşçu, 2000; McNeill, et al., 2004) and corresponds to the prolongation of the Main Marmara Fault

(Roussos & Lyssimachou, 1991; Le Pichon, et al., 2001) west of the Dardanelles Strait (Janin, Rodriguez, Sakellariou, Lykousis, & Gorini, 2018). The southern branch of the North Anatolian Fault, is characterized by ~ a 5 mm·yr^{-1} rate (Le Pichon & Kreemer, 2010), terminates off Skyros Island, and forms the Edremit Trough (Janin, Rodriguez, Sakellariou, Lykousis, & Gorini, 2018).

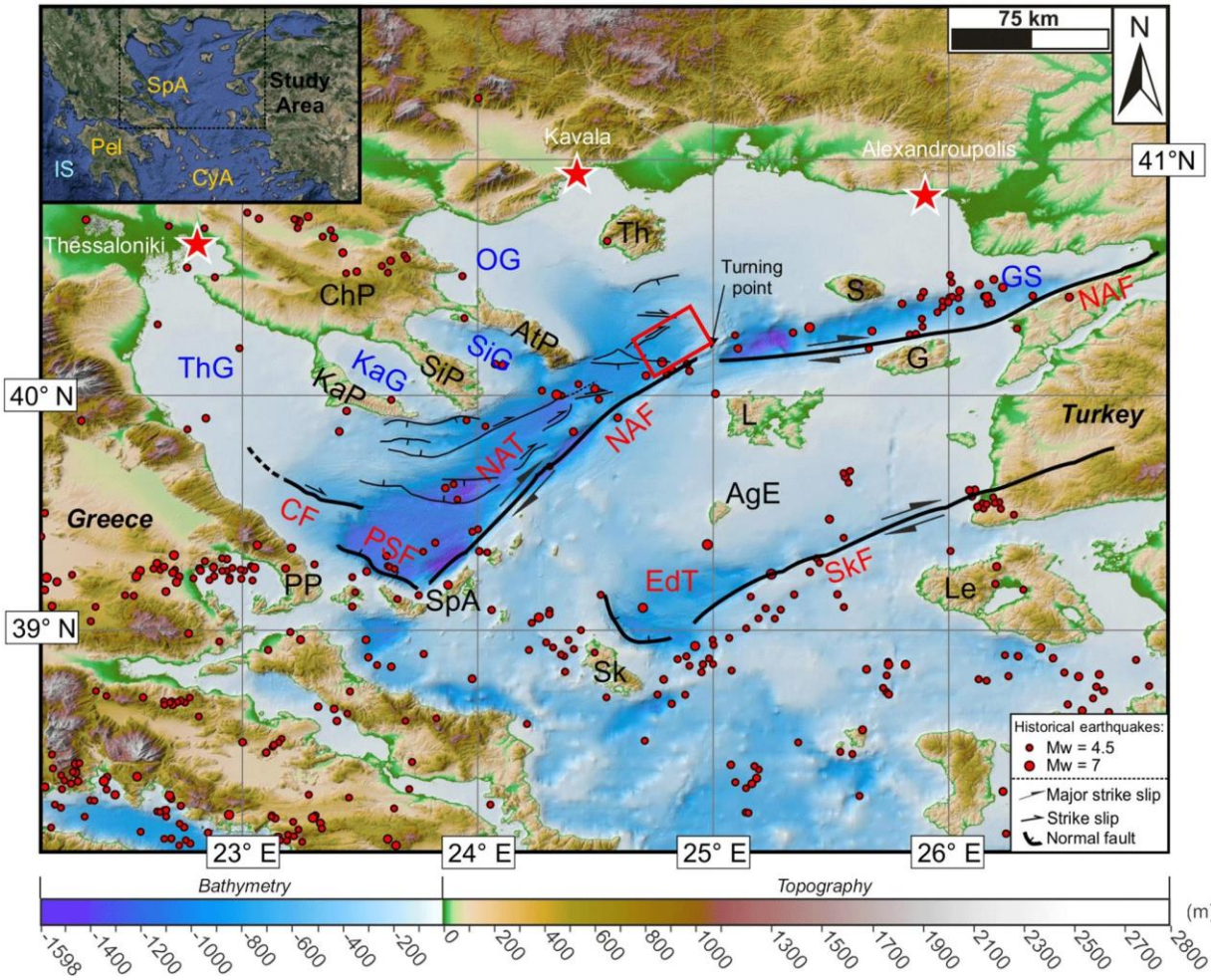

Figure 3. *Morphological map of the major structural elements (after Sakellariou and Tsampouraki-Kraounaki (2016)). The seismic data (red dots) were acquired from USGS and correspond to earthquakes with Mw > 4.5 since January 1st, 1950. The inset map shows the location of the North Aegean Sea. General topography and bathymetry from SRTM30 (Becker et al., 2009) and high–resolution bathymetry (250m) from Sakellariou and TsampourakiKraounaki (2016). Abbreviations: AgE: Agios Efstratios, AS: Aegean Sea, EdT: Edremit Trough, G: Gokceada (Imvros), GS: Gulf of Saros, IS Ionian Sea, KaP: Kassandra Peninsula, L: Lemnos, Le: Lesvos, NAT: North Aegean Trough, NAF: North Anatolian Fault, OG: Orfani Gulf, Pel: Peloponnese, PP: Pelion Peninsula, PSF: Pelion – Skopelos Fault, S: Samothraki, SiG: Sigitikos Gulf, Sk: Skyros, SkF: Skyros Fault, ThG: Thermaikos Gulf (Janin et al., 2018).*

This prolongation of NAF into the Aegean region was accompanied by a change in the tectonic style of deformation in the Aegean Sea, which afterward was strongly controlled by the right and left lateral strike-slip offshore faulting, distributed within the entire region (Mascle & Martin,

1990; Sakellariou, Mascle, & Lykousis, 2013). In particular, the direction of extension in the South Aegean Sea shifted from N–S (Late Miocene) to NE–SW since the Early Pliocene, perpendicular to the Ionian branch of the Hellenic trench (Mascle & Martin, 1990). Thus, the former E–W structures rotated to ENE–WSW direction and progressively obtained characteristics of transcurrent features.

GPS surveys over the last decades in the eastern Mediterranean have been used for the quantification of the deformation of the Aegean Sea (Billiris, et al., 1991; Le Pichon, Chamot-Rooke, Lallemant, Noomen, & Veis, 1995; Davies, et al., 1997; Clarke, et al., 1998; McNeill, et al., 2004). NAF accommodates dextral strike-slip motion at a slip rate of 23 $mm \cdot yr^{-1}$ according to GPS data (Kahle, et al., 2000; McClusky, et al., 2000; Kreemer, Chamot-Rooke, & Le Pichon, 2004; Nyst & Thatcher, 2004; Pérouse, et al., 2012; Müller, et al., 2013; Reilinger, et al., 2006; Le Pichon & Kreemer, 2010). In general, GPS data have confirmed the aforementioned geotectonic model and other main, active processes that are mentioned below (Figure 4), (Papanikolaou, Alexandri, & Nomikou, 2006; Sakellariou, Mascle, & Lykousis, 2013);

- the westward extrusion of Anatolia continental block along the NAF,
- the NNEward subduction of the Eastern Mediterranean lithosphere beneath the Hellenic Arc,
- the SSW – NNE extension of the Aegean back-arc region,
- the eastward movement of the Apulian block converging with the northern Hellenides in the northern Ionian Sea, north of the Kephallonia Fault, and
- the incipient collision with the Libyan promontory south of Crete (Mascle et al., 1999)

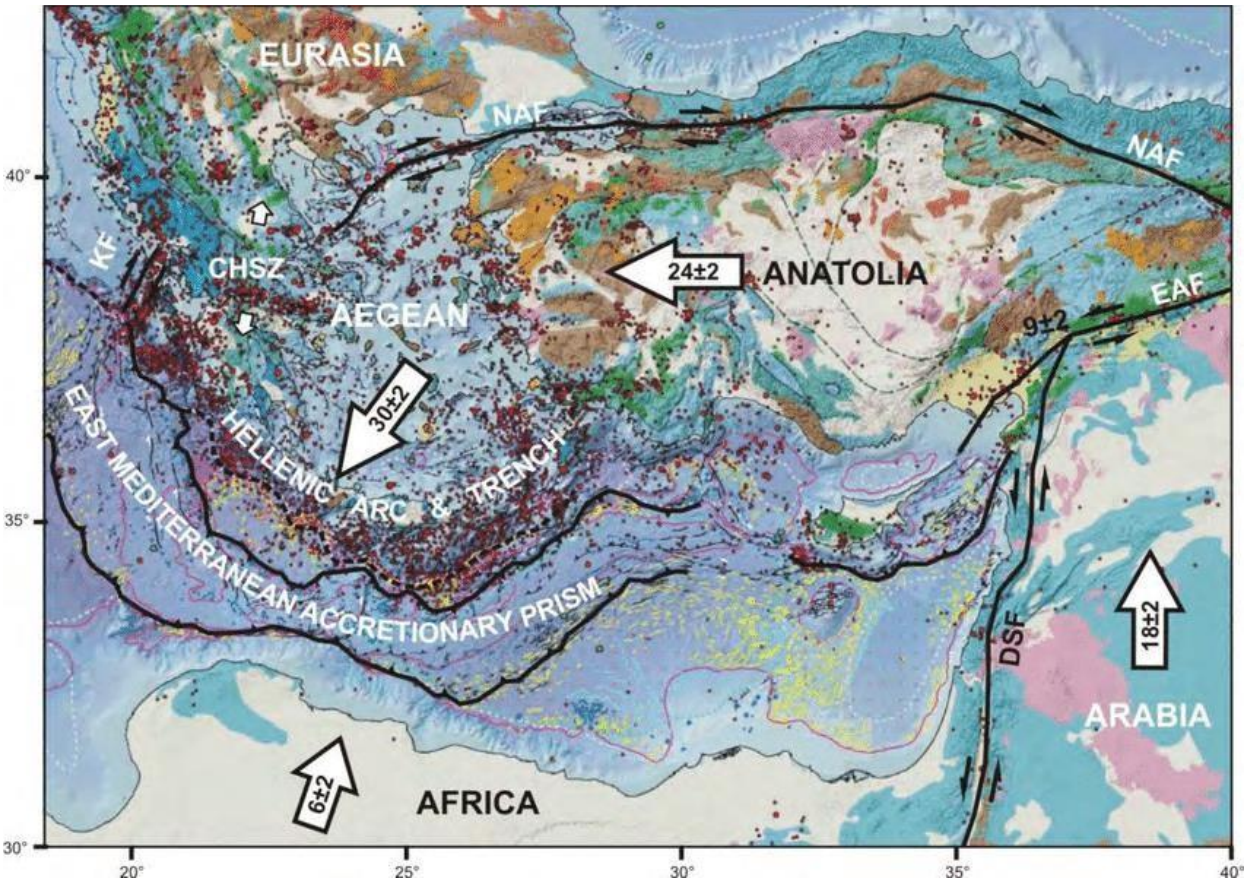

Figure 4. *Morphotectonic map of the East Mediterranean Sea (after Mascle & Mascle, 2012). Black lines correspond to major tectonic boundaries of the Aegean Region. White arrows show GPS horizontal velocities and directions of the distinctive plates with stable Eurasia (after McClusky et al (2000)). Abbreviations: DSF: Dead Sea Fault, EAF: East Anatolian Fault, NAF: North Anatolian Fault, KF: Kephallonia Fault, CHSZ: Central Hellenic Shear Zone (Sakellariou et al., 2013).*

2.2. NORTH AEGEAN BASIN – LIMNOS BASIN – SAROS TROUGH

The North Aegean Basin (NAB) has been considered one of the major expressions of the prolongation of the NAF into the Aegean Sea in the Early Pliocene or Pleistocene (McKenzie, 1970; Dewey & Şengör, 1979; Lyberis, 1984; Armijo, Meyer, Hubert, & Barka, 1999; Papanikolaou, Alexandri, Nomikou, & Ballas, 2002; Papanikolaou, Alexandri, & Nomikou, 2006; Brun, et al., 2016). The NAF created, an approximately 150 kilometers long transtensional basin that forms an almost orthogonal quadrangle that is elongated in a NE–SW direction (Sakellariou, Mascle, & Lykousis, 2013), that developed over a pre-existing Early Tertiary molassic sedimentary basin with up to 6 kilometers thick sediments deposited below the Thermaikos–Sporadhes basin since Middle Miocene (Dermitzakis & Papanikolaou, 1981; Lyberis, 1984; Mascle & Marin, 1990; Papanikolaou, Alexandri, & Nomikou, 2006).

The overall basin marks the northern transform–type tectonic boundary of the expanding Aegean microplate (Mascle & Martin, 1990; Sakellariou, Mascle, & Lykousis, 2013; Sakellariou, et al., 2018). Recent GPS campaigns confirm that the predominant deformation style in the NAB in the north boundary is dextral shear, (Müller, et al., 2013).

NAB is one of the major basins created by the NAF in the northern boundary of the North Aegean and is neighboring to the east with Limnos Basin and more to the east with Saros Trough that both accommodate different characteristics (Figure 5), such as seafloor morphology and tectonic features (Sakellariou, et al., 2018). NAB extends from Pelion Peninsula to Lemnos Island and is composed of numerous sub-basins, including the Sporades Basin, separated by structural highs and shallower ridges (Lyberis, 1984; Sakellariou, et al., 2018). Limnos Basin is located North of Lemnos island and is composed of the 1500 meters Lemnos Deep, and Saros Trough is located between Samothraki and Gokceada Islands, with a narrow, up to 1000 meters deep basin, and extends to the Dardanelles Strait (Mascle & Martin, 1990).

2.3. SKYROS BASIN - EDREMIT TROUGH

The Skyros Basin is a 100 kilometers long feature that has developed along the southern branch of the North Anatolian Fault, in the southern part of the North Aegean and is neighboring to the east with the Edremit Trough (EdT) and Edremit Gulf (EdG) more to the east (Sakellariou, et al., 2022), (Figure 5).

Skyros Basin has a base parallel to the eastern coastline of Skyros Island and its peak at 70 kilometers, where it continues in the narrower and shallower Edremit Trough. The Skyros Basin trends ENE-WSW and is developed southwards and subparallel to the North Aegean Basin. Both accommodate extension and shearing due to the North Anatolian Fault's westward propagation, which breaks into two major branches (McKenzie, 1970; Kreemer, Chamot-Rooke, & Le Pichon, 2004). Recent GPS campaigns confirm that the predominant deformation style in the Skyros Basin–Edremit Trough in the south boundary is also dextral shear, (Müller, et al., 2013).

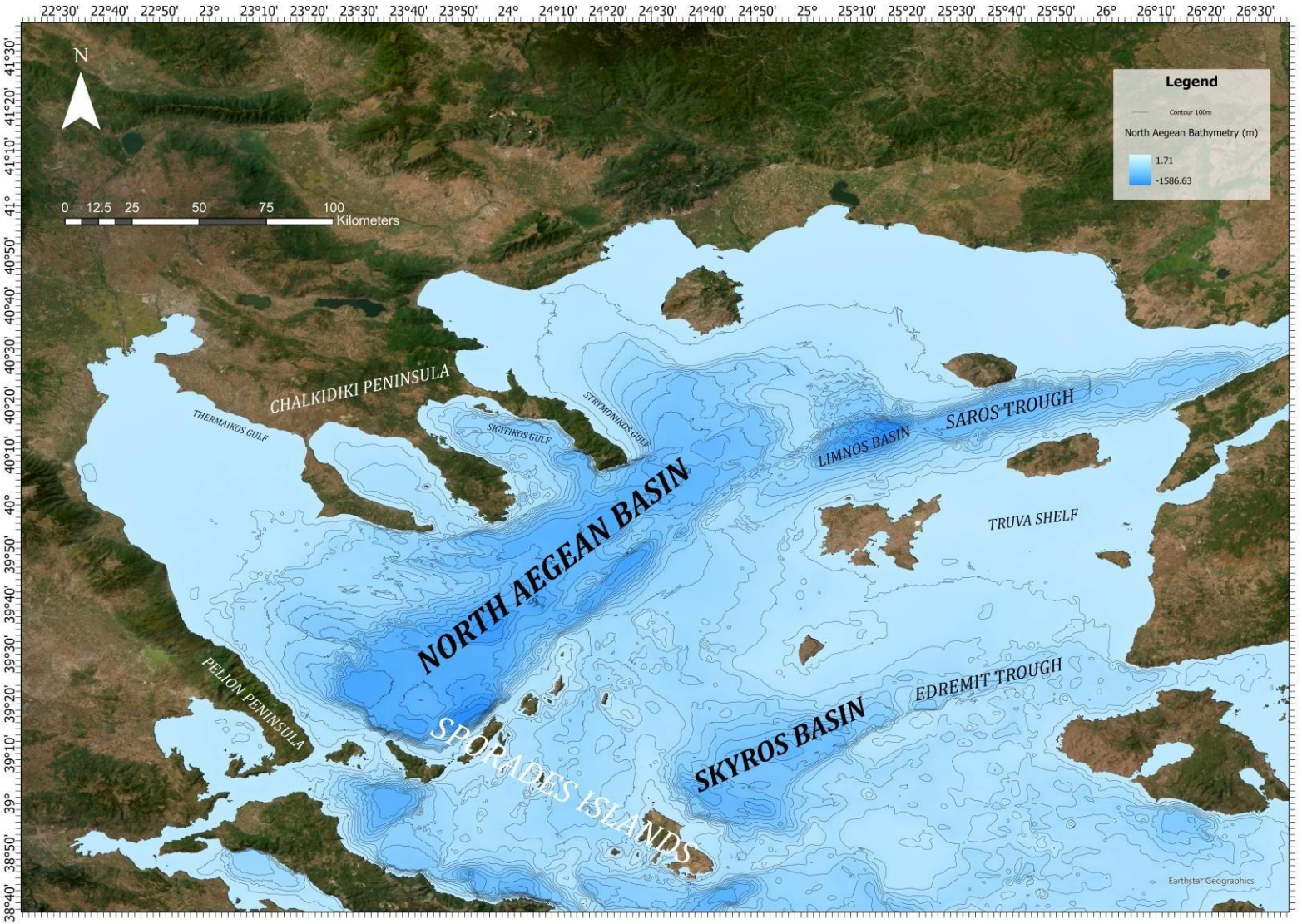

Figure 5. *North Aegean Sea Bathymetric Map with its characteristic locations and deep basins. Black lines correspond to depth contours of 100 meters.*

3. MATERIALS AND METHODS

EMODnet's (European Marine Observation and Data Network), harmonized Digital Terrain Models (DTMs, 2020) for the European Sea regions were used to create a bathymetric map. Those DTMs are divided into tiles and are the products of selected bathymetric survey data sets, composite DTMs, and Satellite Derive Bathymetry (SDB) data, while gaps with no data coverage are completed by integrating the GEBCO Digital Bathymetry. The geodetic system for the grid of the DTMs is chosen as WGS' 84 and the resolution is 105x105 meters.

Two DTM tiles of the areas including the North Aegean and Skyros Basins were selected and downloaded from EMODnet's website and added to ArcGIS. The previous were then merged with Raster Calculator to overlap their data and create a single continuous DTM, which was later clipped by two polygon features of the two study areas. As a result, two clipped DTMs were created, one for the North Aegean Basin and the other one for the Skyros Basin. The data from the DTMs were used to produce a Slope Map (in degrees), a Shaded Relief Map, and Contours through Spatial Analyst Tools in ArcGIS. 3D models of the DTMs were achieved with Global Scene in ArcGIS with varying vertical exaggeration depending on the geomorphological feature highlighted.

Two extensions for ArcGIS were also used; the Benthic Terrain Modeler (BTM) and the Orientation Analysis Tools. The BTM extension includes the Benthic Terrain Classification tool that was applied for the creation of the Synthetic Map. The Orientation Analysis tools extension was utilized to plot rose diagrams of the mean line orientation of line features. Last but not least, the statistical analysis of the Slope Map was accomplished in Microsoft Excel.

4. SUBMARINE GEOMORPHOLOGY

4.1. BATHYMETRY

For a complete interpretation and analysis of the morphological characteristics of the basins, the following were created; Bathymetric Map, Shaded Relief Map, and 3D models. The previous can be found on Pages; 20-22, and 24-25.

4.1.1. NORTH AEGEAN BASIN - NAB

The NAB is not a simple geometric basin with a flat-lying sea bottom. Instead, it has a very complex topographic regime carved by multiple sub-basins developed with different geometric shapes at different water depths and separated by distinct intermediate submarine channels or ridges (Papanikolaou, Alexandri, Nomikou, & Ballas, 2002).

The sub-basins of NAB are the deepest depressions of the basin and are mainly developed at depths larger than 900 meters, the deepest occurring at the SW area of the basin, North of Alonnisos Island, with a depth of 1586 meters. The next deepest basin is located between Kassandra Peninsula and Gioura Island with a maximum depth of 1256 meters. The analysis of the submarine topography by examining the depth distribution chart table, shows an irregular distribution, with the first maximum between 250 and 450 meters depth and a second between 950 and 1150 meters depth (Figure 6). These two highest depth range values correspond to the shallow continental platform outside the basin and to the majority of the deep basinal areas that include the multiple sub-basins, respectively.

Generally, the sub-basins are mostly elongated with a systematic pattern in certain directions, with a small number of round-shaped sub-basins. The prevailing direction of the sub-basins is NE-SW, the same as the direction of the whole NAB.

Starting from SW towards NE of the margin of the basin an alternation of subsided and uplifted areas, both with an elongated shape is evident with the aforementioned direction of NE-SW (Figure 10). There is a significant difference in the geometry of the basin between the SE margin (Sporades and Limnos), which presents a NE-SW direction and an average topographic difference of 800-1000 meters, and the NW margin (Chalkidiki, Thasos), which is not rectilinear but of rectangular shape, created by the Sigitikos and Strymonikos gulfs on both sides of the Mt. Athos Peninsula in the north and the Thermaikos Gulf in the northwest (Papanikolaou, Alexandri, Nomikou, & Ballas, 2002).

The Sigitikos Gulf has a highly prominent asymmetric seafloor morphology, which is defined by steep submarine cliffs near the Athos Peninsula. The Strymonikos Gulf has a relatively geometric form, trends NW-SE, and a maximum depth of 900 meters that gradually increases to 200 meters. The Thermaikos Gulf presents a much more complex pattern, with few major channels and numerous smaller ones, developed in the NW-SE and E-W direction, starting from depths of 1000-1200 meters and entering the continental platform in the form of finger-type undulations at depths less than 400 meters (Papanikolaou, Alexandri, Nomikou, & Ballas, 2002). Thus, the above NW-SE morphological direction along the NW margin of the basin is almost parallel to the direction of the peninsulas of Chalkidiki (Kassandra, Sithonia, Athos) and also almost parallel to the direction of the SW margin of the basin, which is running very close to the eastern Skopelos coast and continues northwestward parallel to the coast of the Eastern Pelion Peninsula.

Moreover, the submarine ridge between Thasos and Limnos, which forms the NE boundary of the basin, is also characterized by a general NW-SE direction. In the continental slopes of the Thermaikos Gulf south of the Kassandra Peninsula, many submarine ridges and valleys are observed trending E-W.

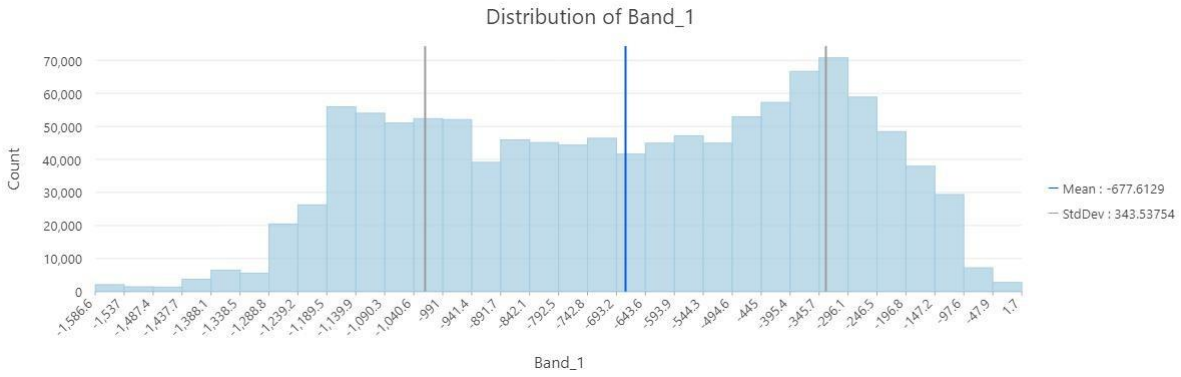

Figure 6. *Distribution Chart of the Bathymetric Data of the North Aegean Basin area.*

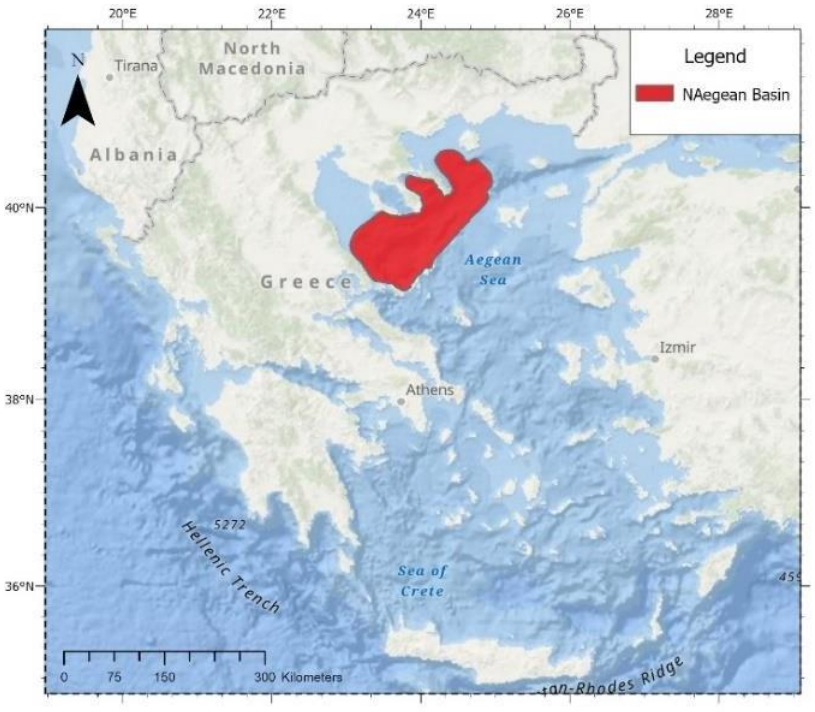

Figure 7. *Location and the area of the North Aegean Basin.*

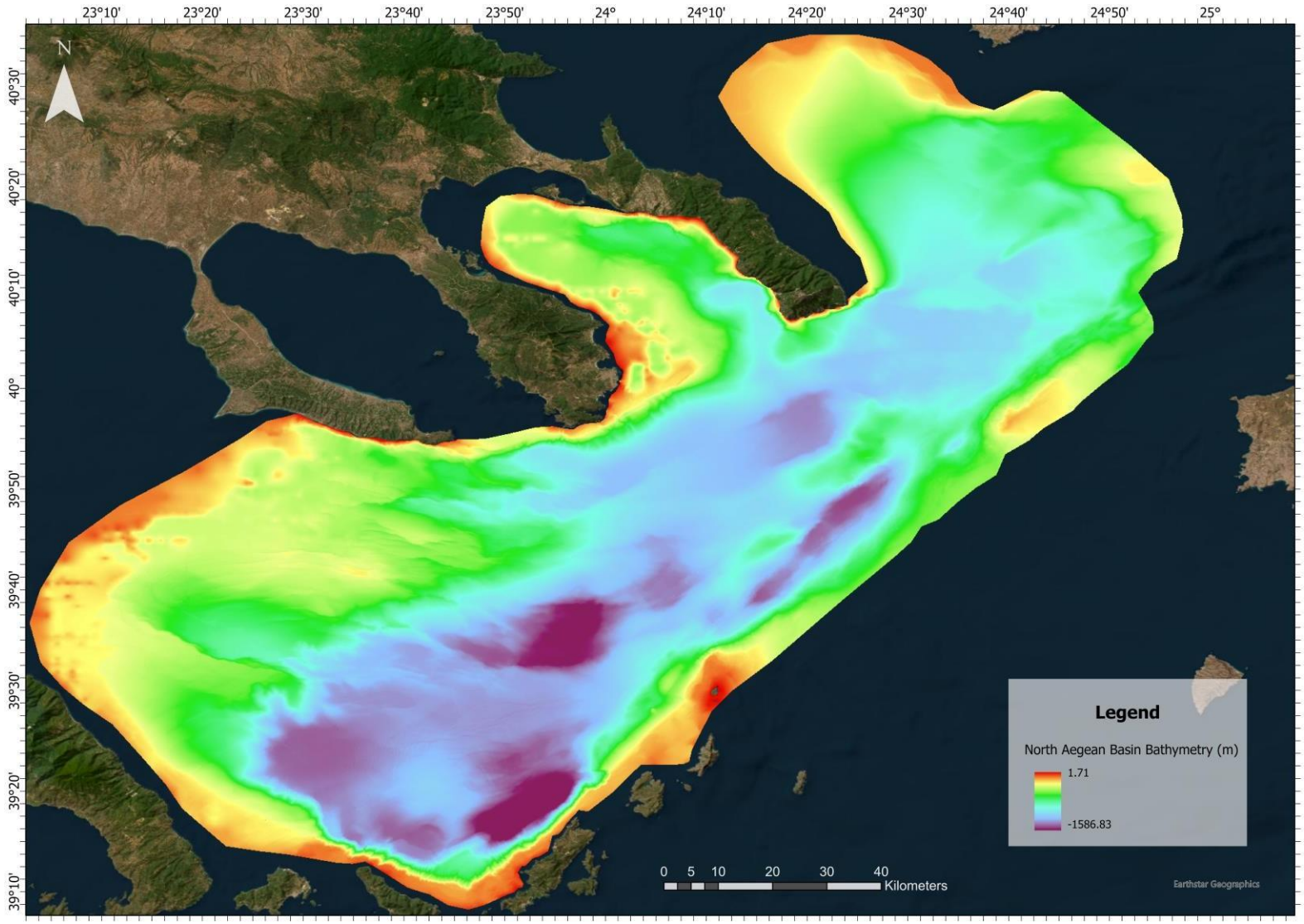

Figure 8. *Bathymetric Map of the North Aegean Basin.*

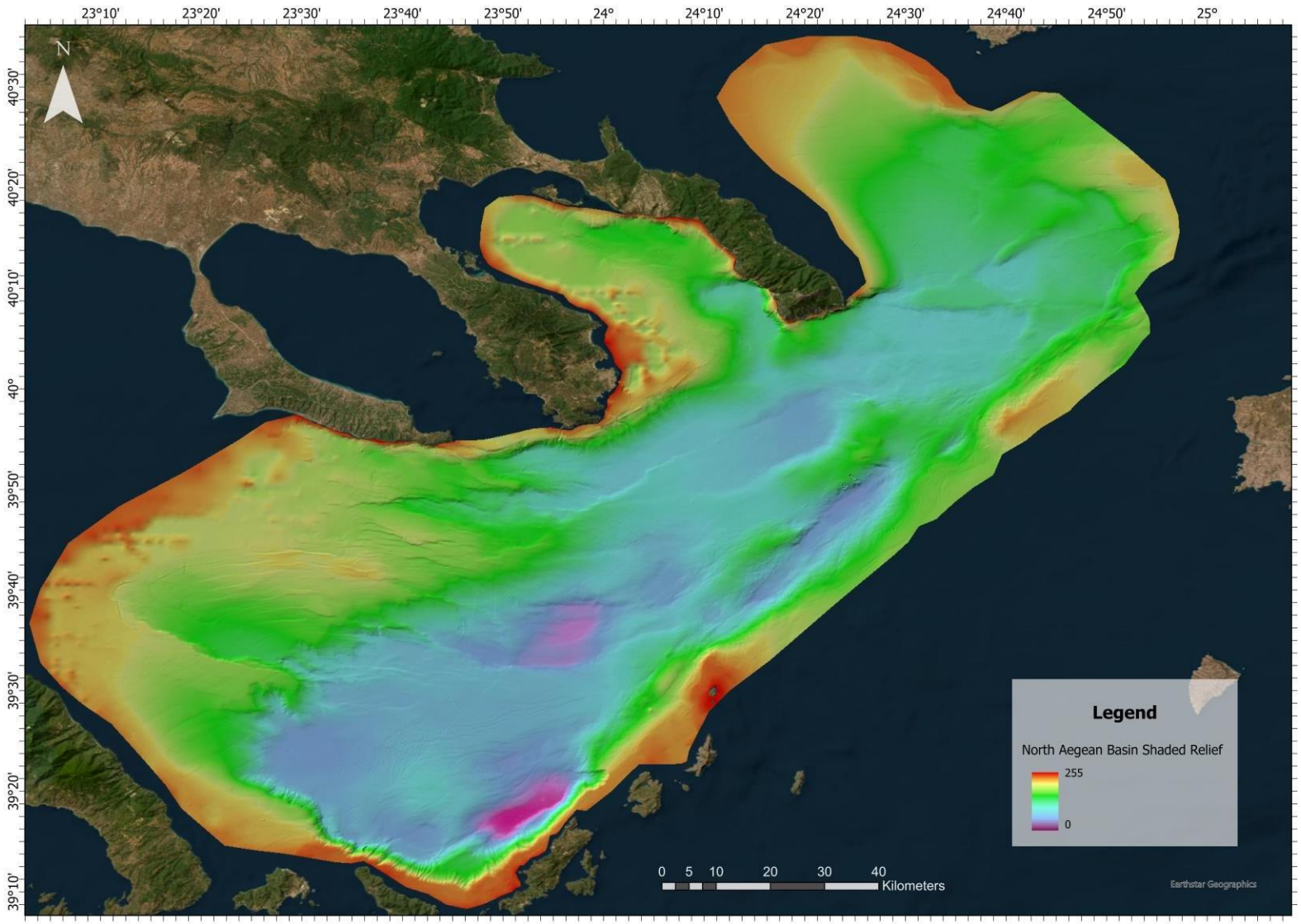

Figure 9. *Shaded Relief Map of the North Aegean Basin, with a traditional Hillshade type.*

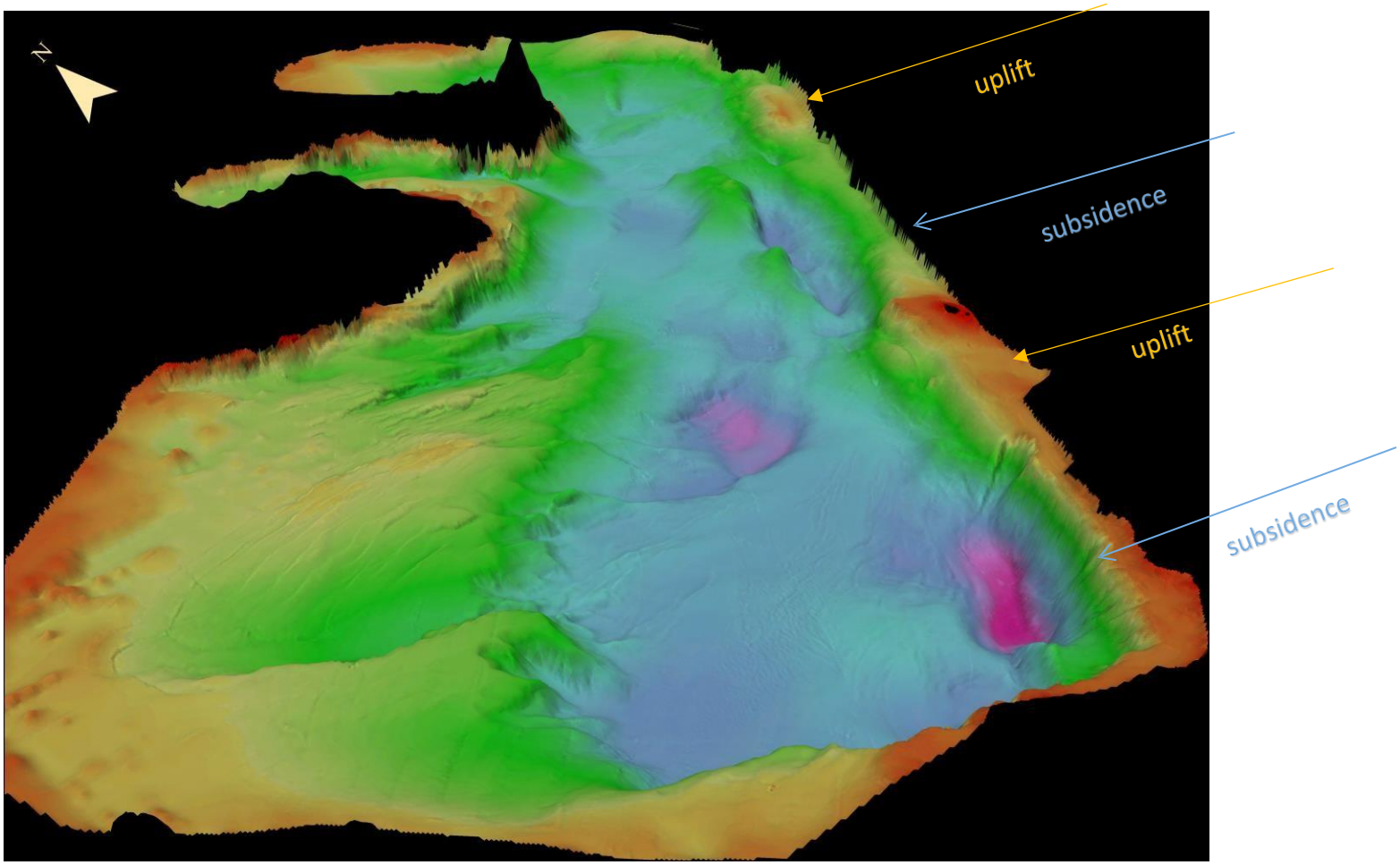

Figure 10. *3D view of the North Aegean Basin with highlights of the subsided and uplifted areas with a vertical exaggeration of 7.*

4.1.2. SKYROS BASIN

The bathymetric map of Skyros Basin shows a rather geometric triangular basin (Papanikolaou, et al., 2019) with a general trend in the ENE-WSW direction and depths varying from 600 to 1050 meters (Figure 13). The width of the basin changes abruptly furthering away from Skyros, where it narrows down and continues towards the Turkish coastlines. A change in the basin's depth and direction is also observed at the transition point. The dominant direction of several sub-basins changes from an NW-SE direction parallel to the Skyros Island coastline, to an E-W direction at the central sub-basins, and an ENE-WSW direction at the eastern sub-basins.

The eastern part of the basin is shallower than the western part, with the western part being 1060 meters deep and the eastern being around 900 meters deep. The maximum width of the overall basin is around 40 kilometers along the maximum length of the NW-SE oriented westernmost sub-basins, whereas immediately to the east the width gradually diminishes down to 10 kilometers. The analysis of the submarine topography by examining the depth distribution chart table shows an irregular distribution, with the first maximum between 230 and 400 meters depth and a second between 760 and 830 meters depth (Figure 11). These two highest depth range values correspond to the continental platform outside the basin and to the majority of the basinal areas that include the multiple sub-basins, respectively.

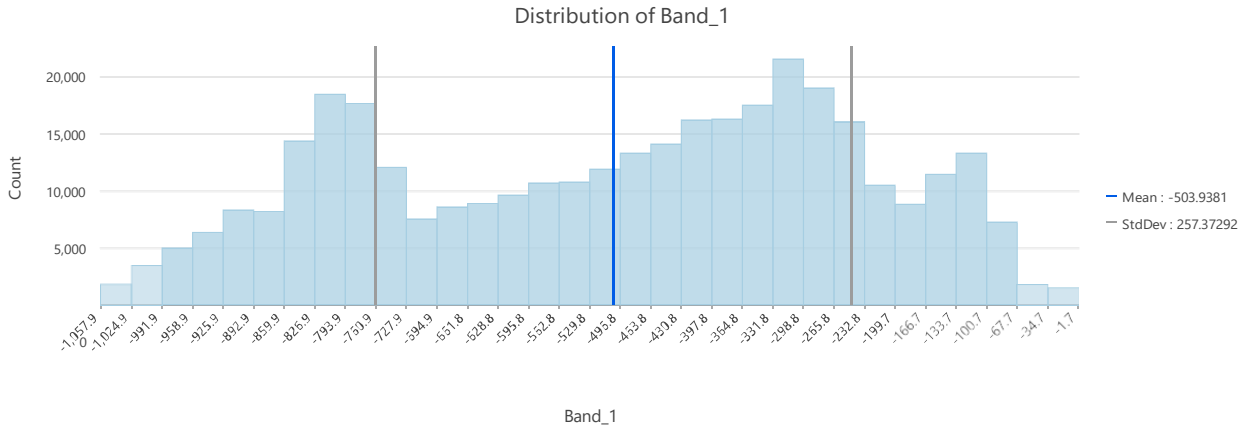

Figure 11. *Distribution Chart of the Bathymetric Data of the Skyros Basin area.*

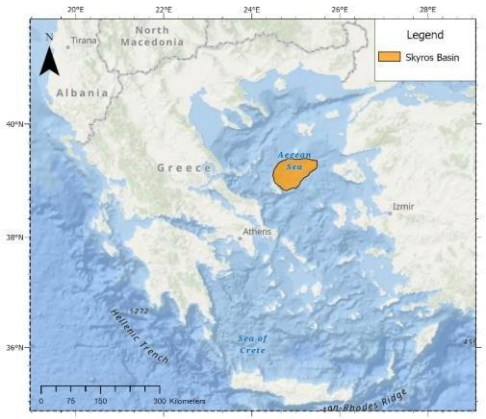

Figure 12. *Location and the area of Skyros Basin.*

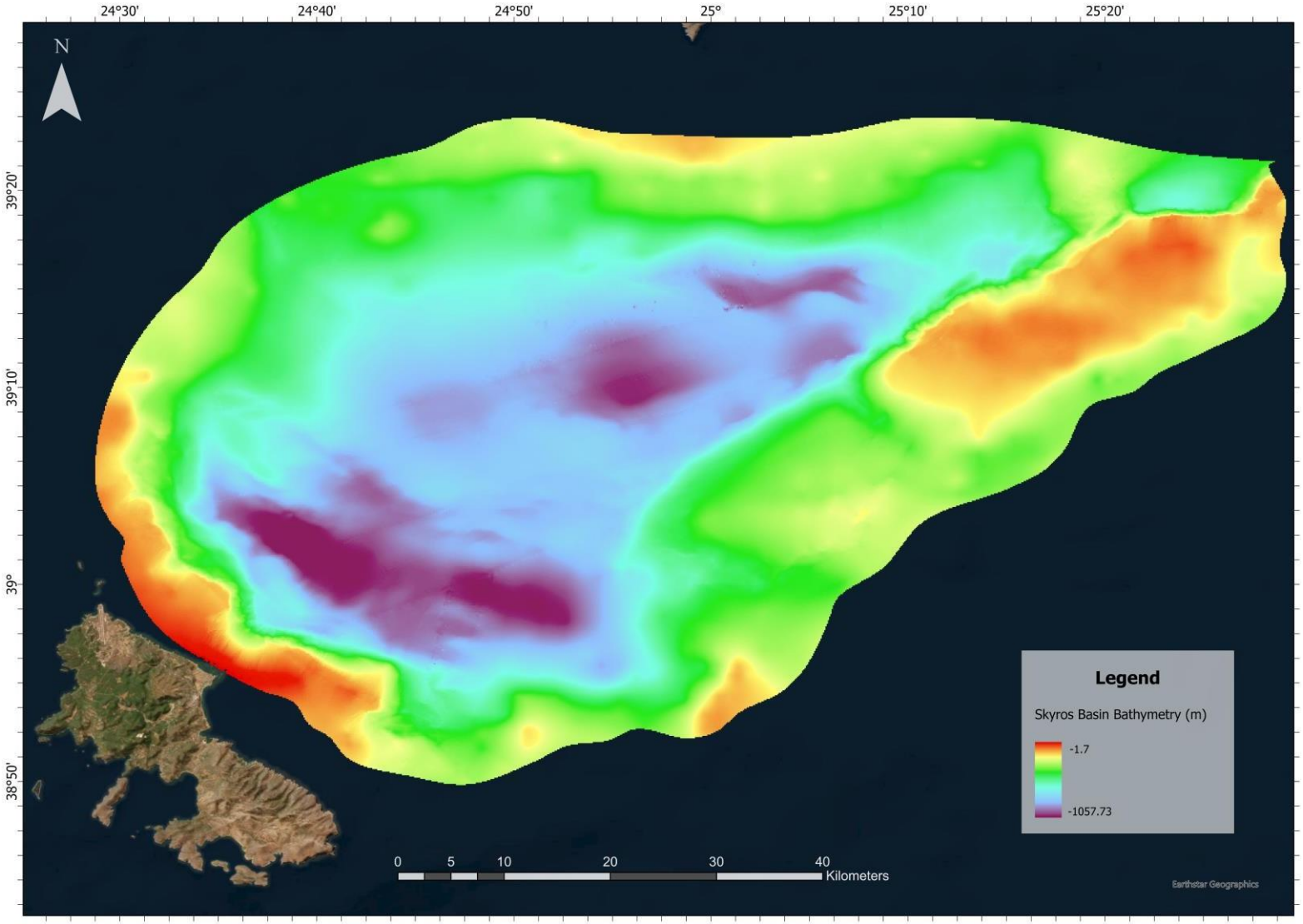

Figure 13. *Bathymetric Map of the Skyros Basin.*

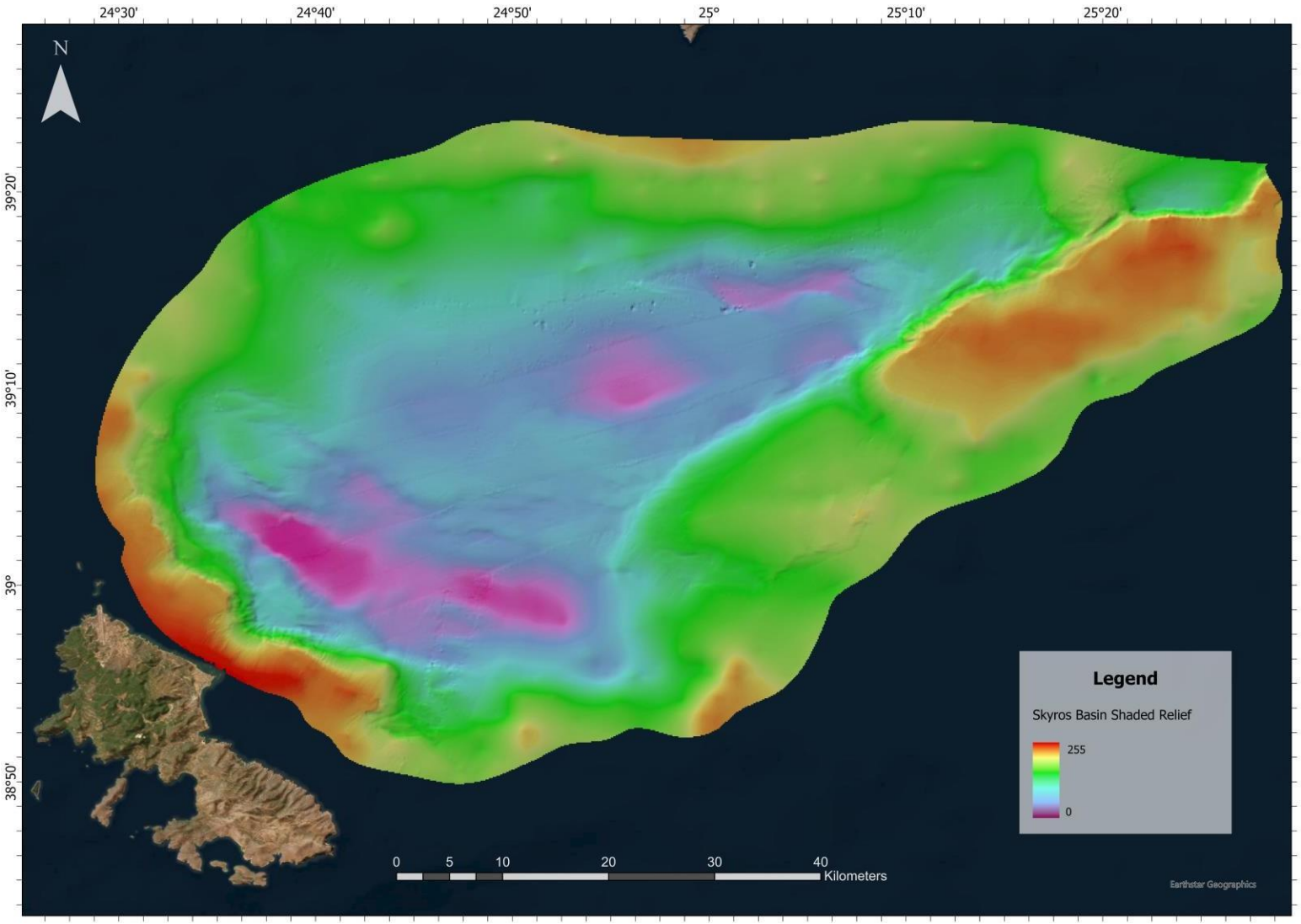

Figure 14. *Shaded Relief Map of the Skyros Basin, with a traditional Hillshade type.*

4.2. CANYONS

4.2.1. NORTH AEGEAN BASIN - NAB

A small number of canyons appear on the slopes of the North Aegean Basin. The north-western margin of the Trough is dissected by several failure scars, associated with short gullies (Sakellariou, et al., 2022). Three longer canyons occur on this margin as seen below in Figure 15. They are 20-30 kilometers long, they initiate at the upper part of the slope, at a depth of between 400-700 meters, and can be traced downslope and on the seafloor of the Basin, following the directions of the main tectonic lines, with the mean direction being ENE.

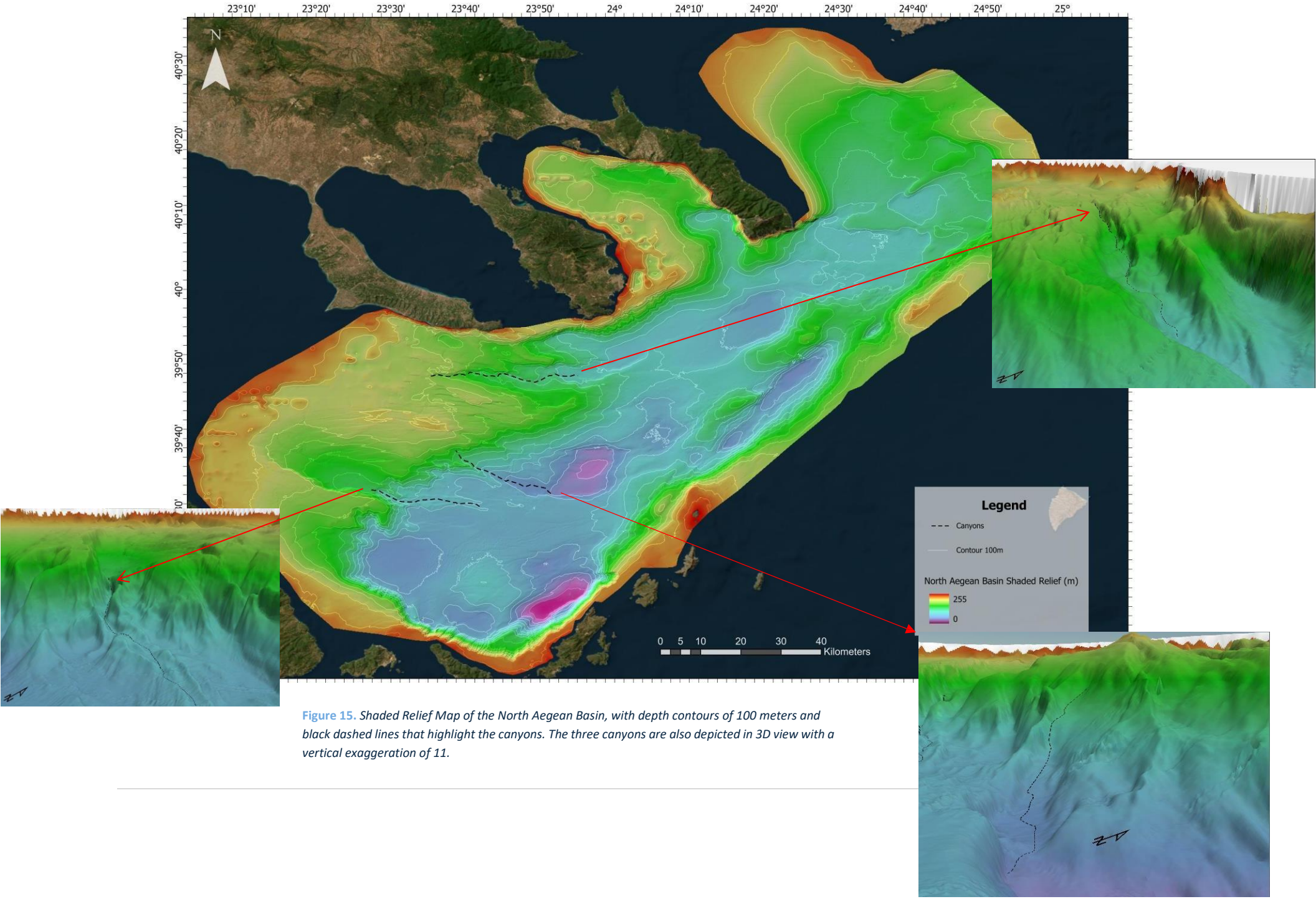

Figure 15. *Shaded Relief Map of the North Aegean Basin, with depth contours of 100 meters and black dashed lines that highlight the canyons. The three canyons are also depicted in 3D view with a vertical exaggeration of 11.*

4.3. SLOPE DISTRIBUTION

The slope distribution map was made using the bathymetric data. The results of this slope analysis are presented on the slope distribution maps below (Figure 17; Figure 19). The slope distribution map displays the distribution of slope values within the studied area categorized into five different classes: (1) areas with a mean morphological slope of 0-1°, (2) areas with 1-5°, (3) areas with 5-10°, (4) areas with a mean morphological slope of 10-20° and (5) areas > 20°. This classification of the slope's value allows for a better distinction of the zones where there is an abrupt change of slope, which usually reflects the position of active tectonic structures, in contrast with zones with a negligible change of slope (Papanikolaou, Alexandri, Nomikou, & Ballas, 2002).

Additionally, the area covered by each class was calculated as percentages. This was achieved by multiplying the count of all the pixels of the raster file with the dimensions of one pixel of the raster file and dividing them by 1000000 for square kilometers, and then converting the square kilometers to percentages. The results are depicted in Figure 16 and Figure 18.

4.3.1. NORTH AEGEAN BASIN - NAB

The class value with a range of 1-5° dominates the area percentages, mostly representing the continental platform and basinal areas, followed by the range of 5-10° which mostly represents the continental slope, followed by the range of 0-1° which represents the flat part of the continental platform and the flat part of the basin, followed by slopes with a range of 10-20° that depicts the steep slopes, and lastly the values of slopes above >20° that are connected to active tectonic zones.

The highest slope values (>20°) create zones with linear shapes and the same direction as discussed in the previous sub-chapter, with a striking appearance on the slopes that are parallel to Chalkidiki's peninsula coast, and the SW corner of the basin.

NORTH AEGEAN	SLOPE STATISTICS		
	Area (km2)	Area %	
1-5°	6399	53.143427	1
5-10°	2560	21.260693	2
>20°	419	3.4797774	5
TOTAL AREA	12041	100	

Figure 16. *Table that includes statistics about the Slope classes of the North Aegean Basin.*

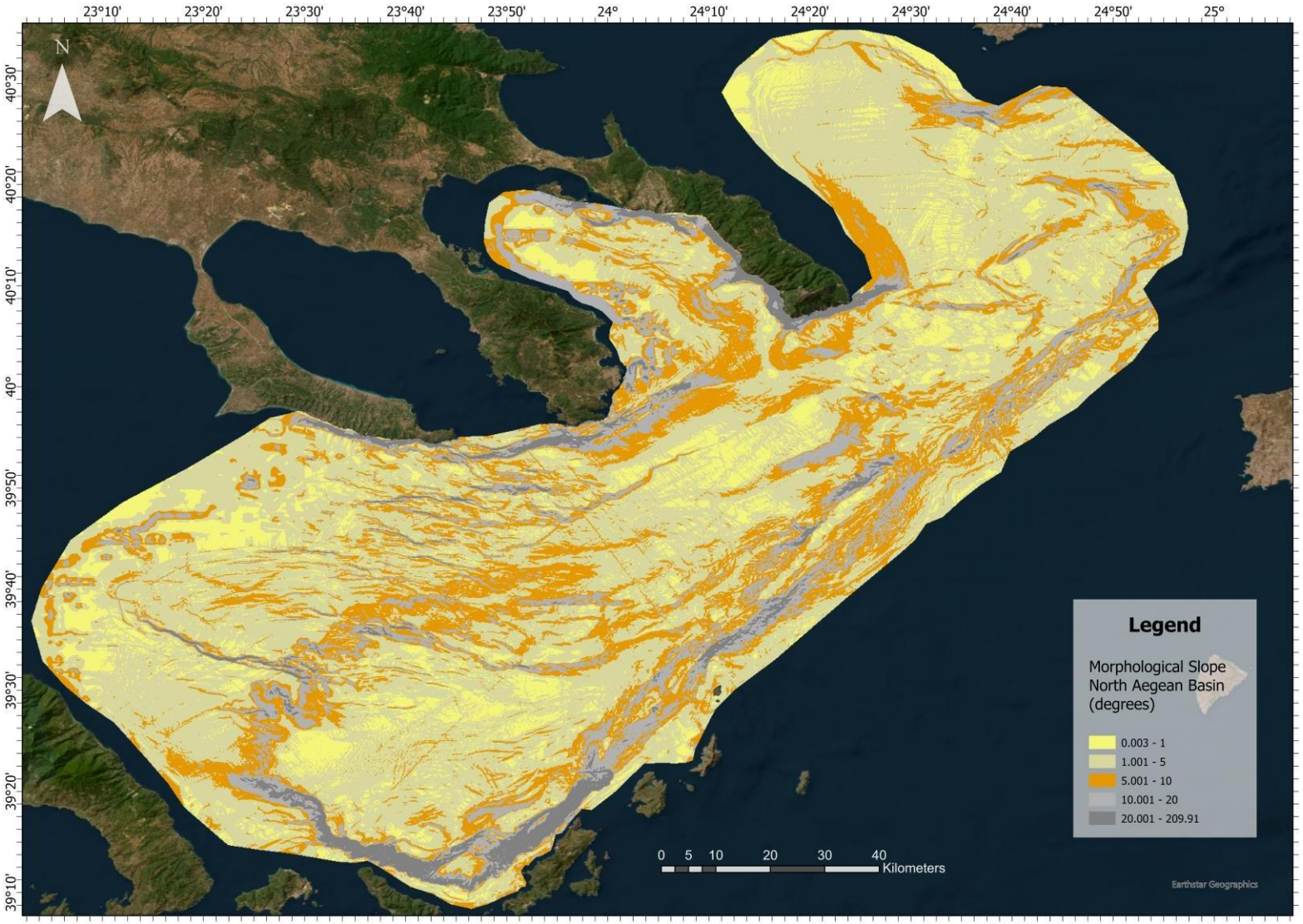

Figure 17. *Morphological Slope Distribution Map (in degrees) of the North Aegean Basin, classified into 5 classes.*

4.3.2. SKYROS BASIN

The same pattern as seen above in the NAB is repeated, as far as area percentages go. The highest slope values have a linear shape and are observed on the eastern side of the basin with ENE-WSW direction and on the western side of the basin parallel to Skyros's coastline, with multiple steep zones of NW-SE direction.

SKYROS	***SLOPE***	***STATISTICS***	
	Area (km2)	Area %	
0-1°	276	7.5803351	**3**
1-5°	2276	62.510299	**1**
5-10°	773	21.230431	**2**
10-20°	243	6.6739907	**4**
>20°	73	2.0049437	**5**
TOTAL AREA	3641	100	

Figure 18. *Table that includes statistics about the Slope classes of the Skyros Basin.*

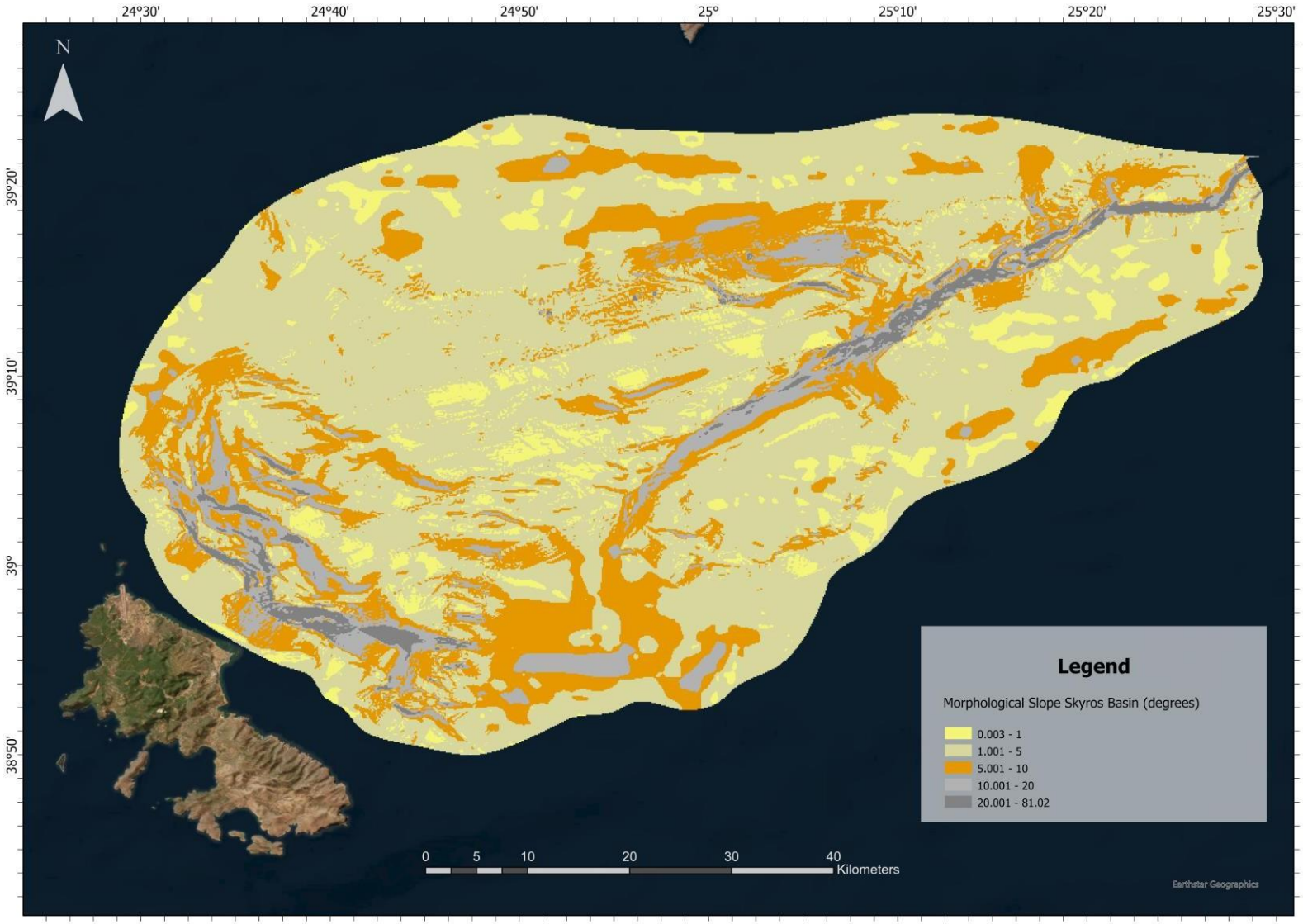

Figure 19. *Morphological Slope Distribution Map (in degrees) of the Skyros Basin, classified into 5 classes.*

4.4. MORPHOLOGICAL DISCONTINUITIES

Morphological discontinuity interpretation is possible based on the previously presented maps, showcasing the major and the minor discontinuities (Figure 21), (Figure 23). The abrupt change of low values of slope to high values of slope marks the major morphological discontinuity, while the abrupt change of high values of slope to low values of slope marks the minor morphological discontinuity.

4.4.1. NORTH AEGEAN BASIN – NAB

The edge of the continental platform outlines the shape of the basin, which is marked by a major morphological discontinuity of more than 10° difference in morphological slope between the continental platform and the continental slope at depths of 200-500 meters (Figure 20). It is characteristic that the boundary of the basin resembles an orthogonal shape in the SW and the SE margins, which consists of multiple segments of major morphological discontinuities in succession to each other, in contrast to the disrupted NW and NE margins, which contain multiple major morphological discontinuities of smaller scale. The deep basins are schematically represented on this map by their flat basinal areas occurring at depths between 900 and 1600 meters. Their distribution delineates the most depressed areas of the basin.

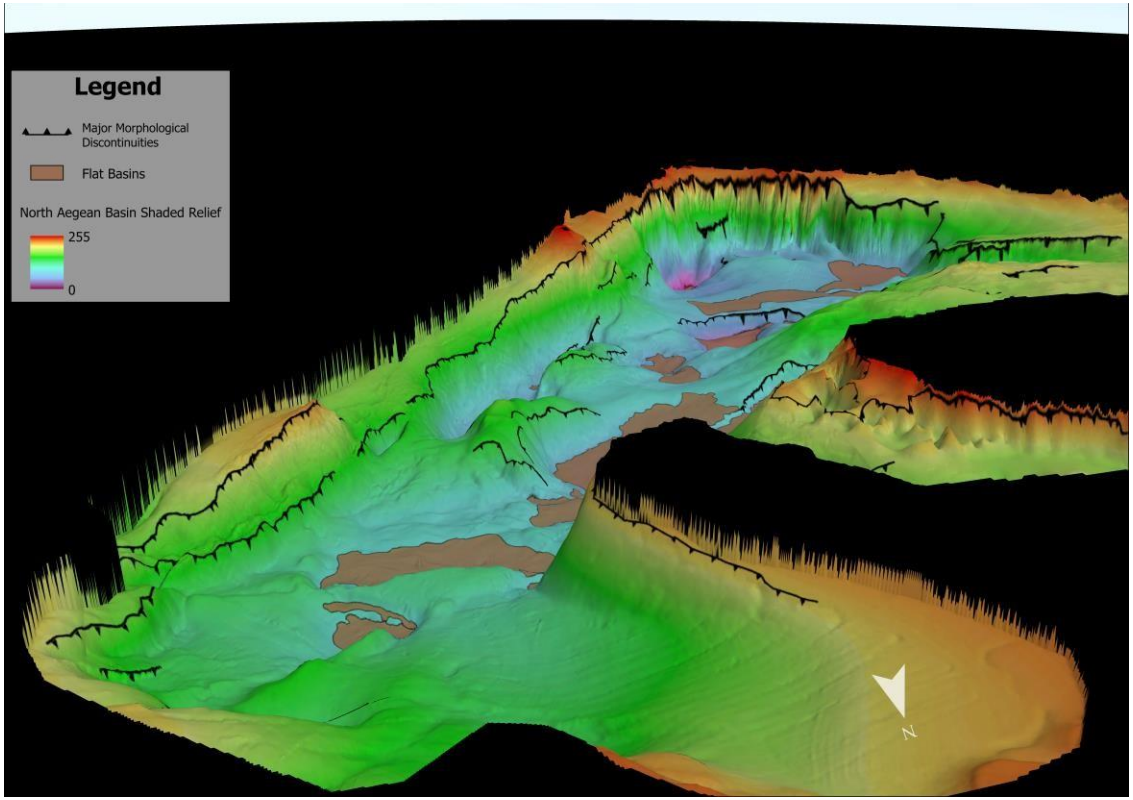

Figure 20. *3D view of the major morphological discontinuities, and the flat part of the basin of the North Aegean Basin, with a vertical exaggeration of 11.*

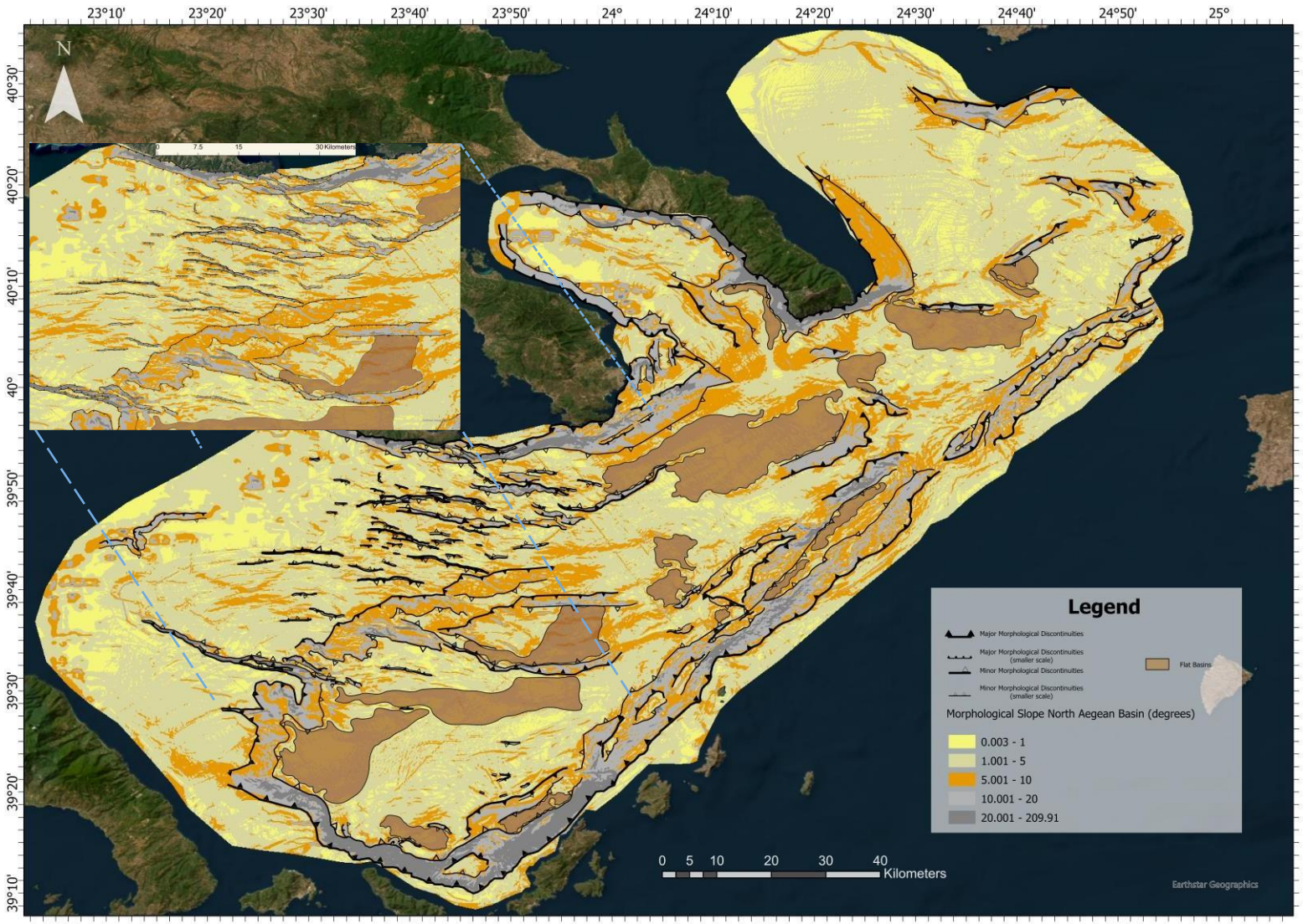

Figure 21. *Morphological Discontinuities Map of the North Aegean Basin.*

4.4.2. SKYROS BASIN

A major morphological discontinuity appears in the SW and SE parts of the basin. Those major aforementioned morphological discontinuities have a NE-SW and ENE-WSW direction accordingly, separating the continental platform from the continental slope at depths between 200 and 400 meters, with more than 10° difference in morphological slope as in the North Aegean Basin previously (Figure 22). Meanwhile, at the rest of the basin, discontinuities that are observed are of a smaller scale, mainly in the deeper flat parts of the previous. The flat basinal areas occur at depths between 800 and 1050 m.

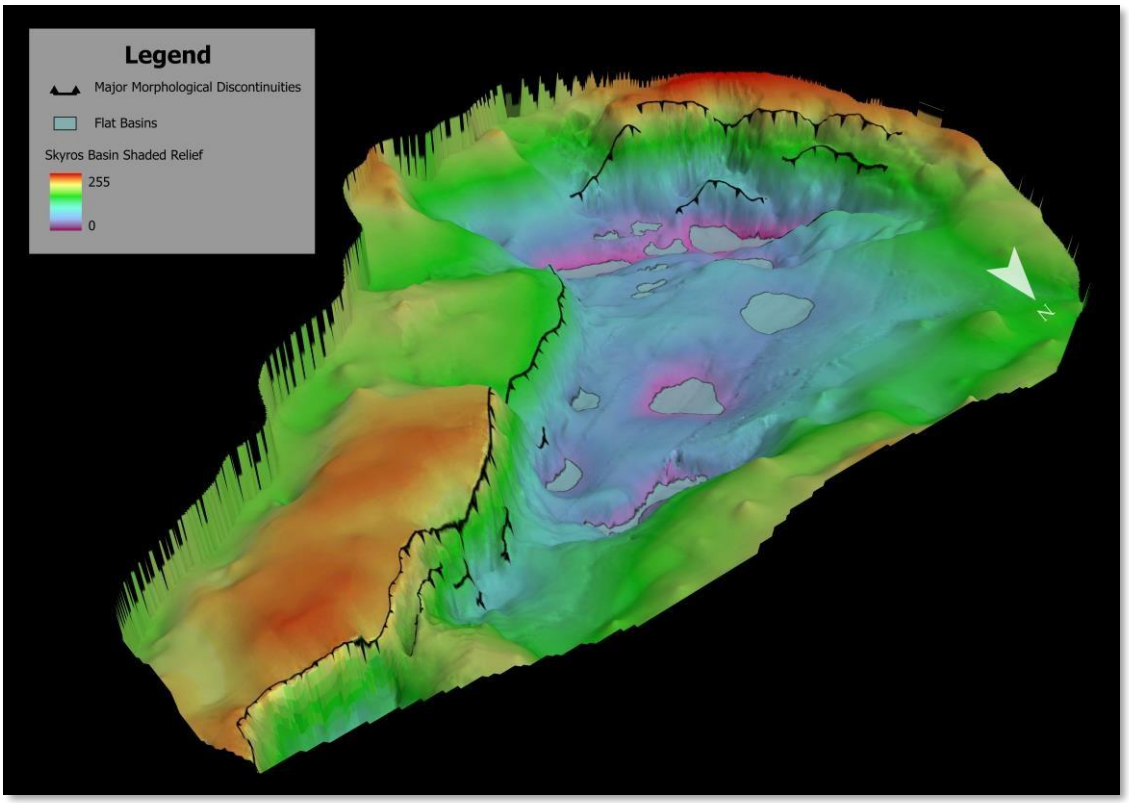

Figure 22. *3D view of the major morphological discontinuities, and the flat part of the basin in the Skyros Basin, with a vertical exaggeration of 11.*

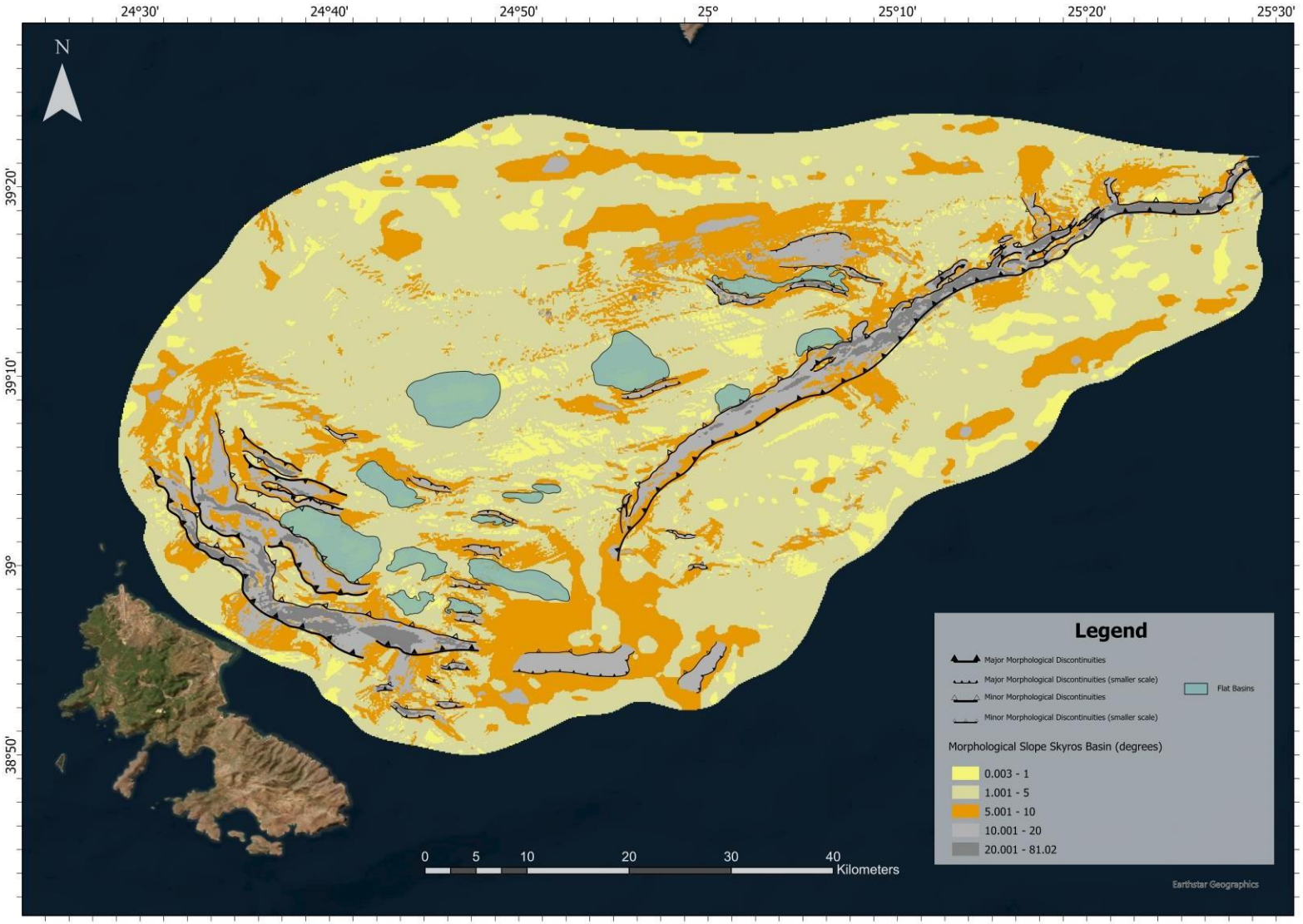

Figure 23. *Morphological Discontinuities Map of the Skyros Basin.*

5. MORPHOTECTONIC AND GEOMORPHOLOGICAL ANALYSIS

5.1. MORPHOTECTONIC ANALYSIS

The overall morphology of the sea bottom is controlled by the plethora of faults included in the morphotectonic maps (Figure 26), (Figure 29). In most cases, they have been traced following the lines separating high slope values from small ones and thus they are usually traced at the foothills of the submarine mountains, separating the areas of relative uplift from the areas of relative subsidence (Papanikolaou, Alexandri, Nomikou, & Ballas, 2002). In some other cases, the major faults are traced along lines that systematically affect the topography, not only as abrupt changes of the morphological slope but also as a change of direction of the margins or the submarine channels and ridges (Papanikolaou, Alexandri, Nomikou, & Ballas, 2002). Major faults from the morphotectonic map, are more than 10 kilometers long, while there are some minor faults of smaller scale too.

The mean orientation of each segment of the major fault lines and the smaller scale fault lines separately was calculated and plotted on a rose diagram, for a statistical approach.

5.1.1. NORTH AEGEAN BASIN - NAB

The major fault lines of the basin have three prominent mean linear orientations; NE-SW, NW-SE, and E-W (Figure 24). On the other side, minor fault lines have a mean linear orientation close to E-W (Figure 25) and are also observed as secondary structures within the basin, delineating some marginal zones of the deep sub-basinal areas or in the continental slope. However, the NE-SW mean linear orientation seems to have the biggest length faults, whereas the NW-SE mean linear orientation has a higher amount of number of faults.

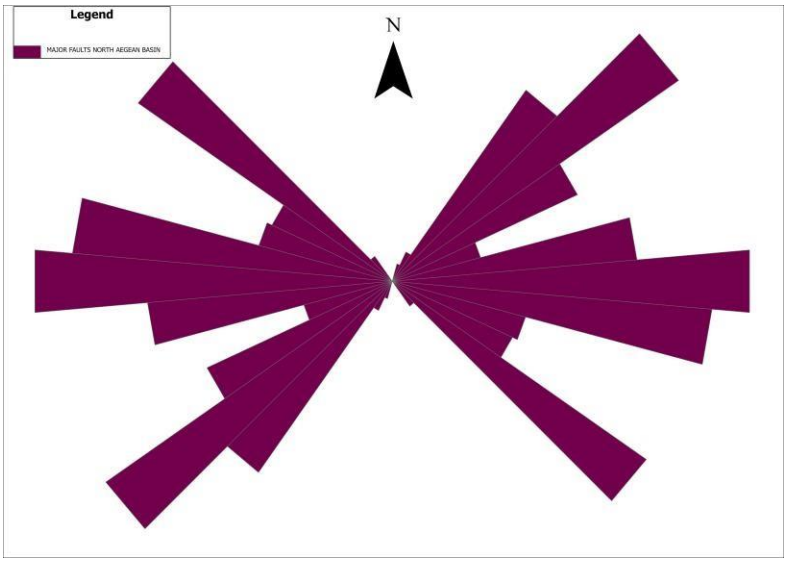

Figure 24. *Rose diagram of the mean line orientation of the major faults in the North Aegean Basin*

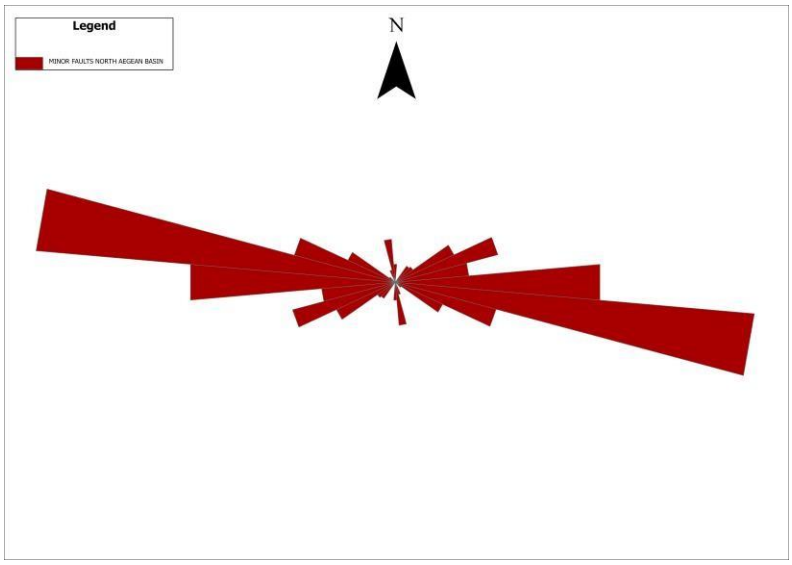

Figure 25. *Rose diagram of the mean line orientation of the minor faults in the North Aegean Basin.*

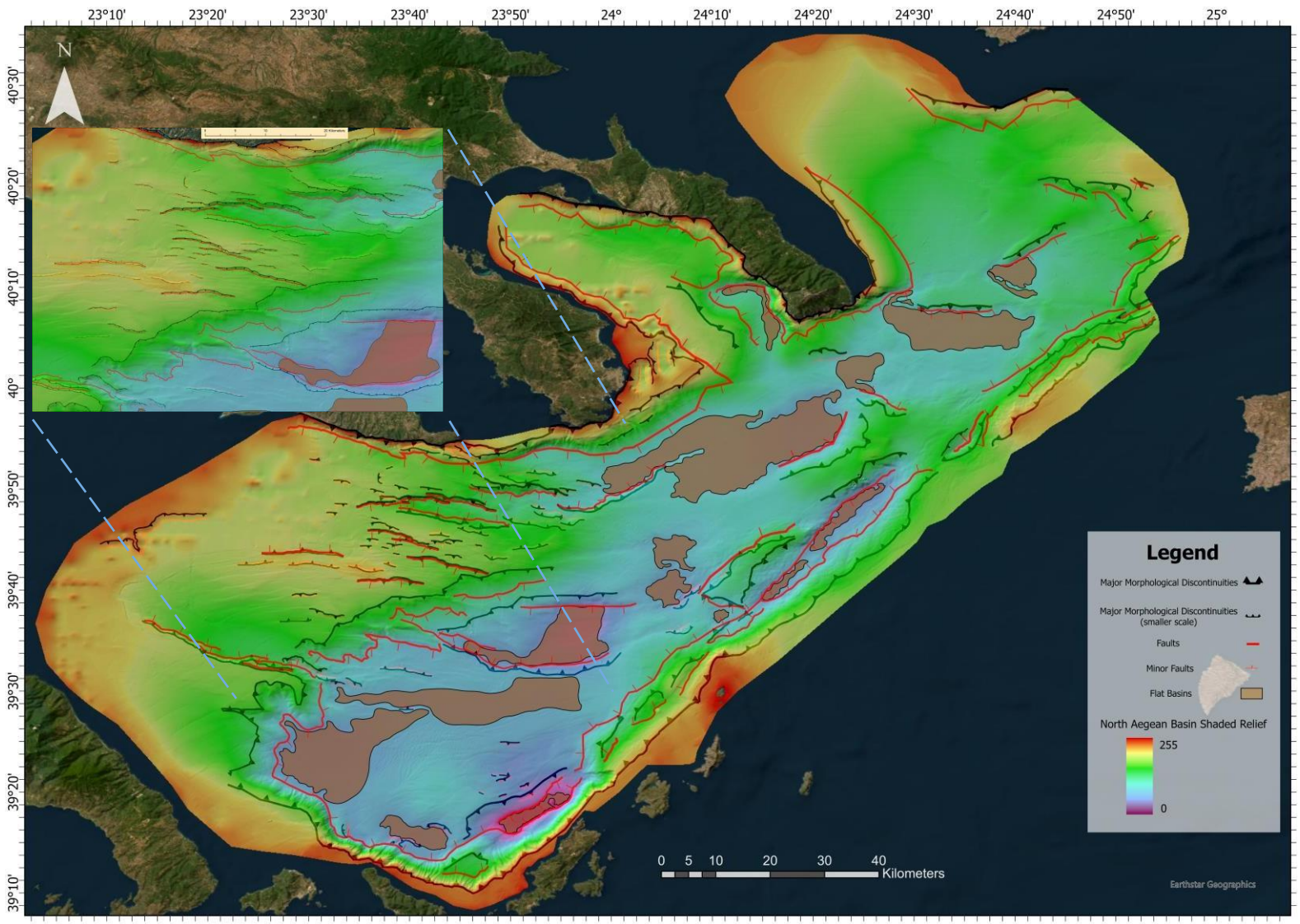

Figure 26. *Moprhotectonic Map of the North Aegean basin, with faults, major morphological discontinuities, and the flat part of the basin.*

5.1.2. SKYROS BASIN

Through the morphotectonic map, two major fault structures are observed in Skyros Basin near the margin of the basin, and some minor faults in the central part. The first one is located on the SW side of the basin with the most prominent mean linear orientation of NE-SW, and the second one the SE side of the basin with the most prominent mean linear orientation of WNW-ESE (Figure 28). The minor fault structures are located near the central area of the basin, have an E-W mean linear orientation, and delineate some marginal zones of the deep sub-basinal areas (Figure 27). As seen in the NAB the NE-SW mean linear orientation contains the biggest length faults, but the NW-SE orientation has a higher amount of number of faults.

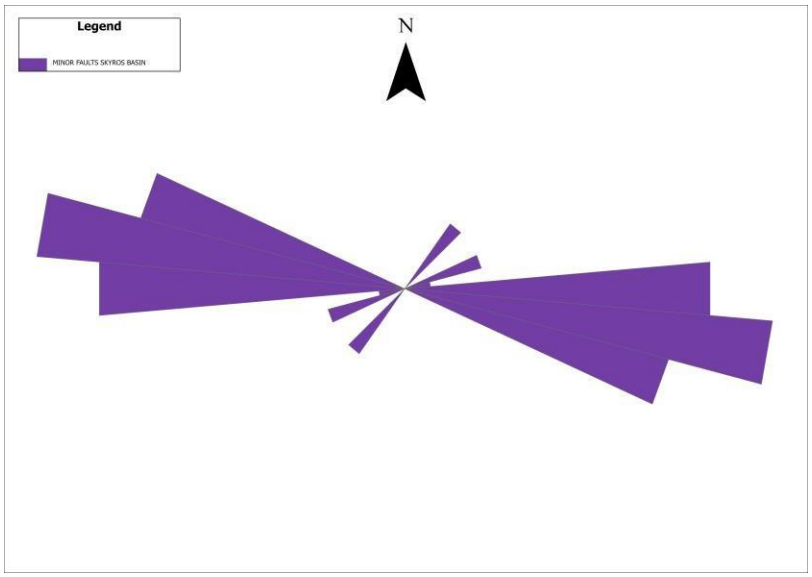

Figure 27. *Rose diagram of the mean line orientation of the minor faults in the Skyros Basin.*

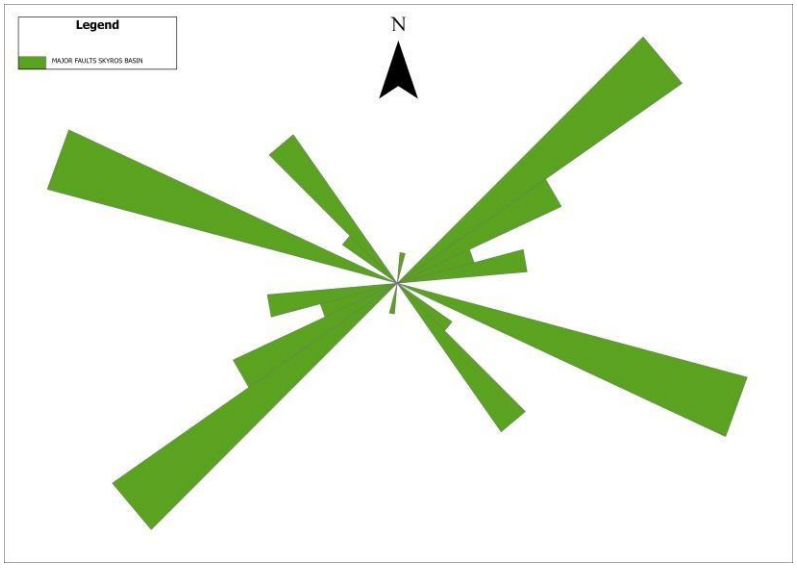

Figure 28. *Rose diagram of the mean line orientation of the major faults in the Skyros Basin.*

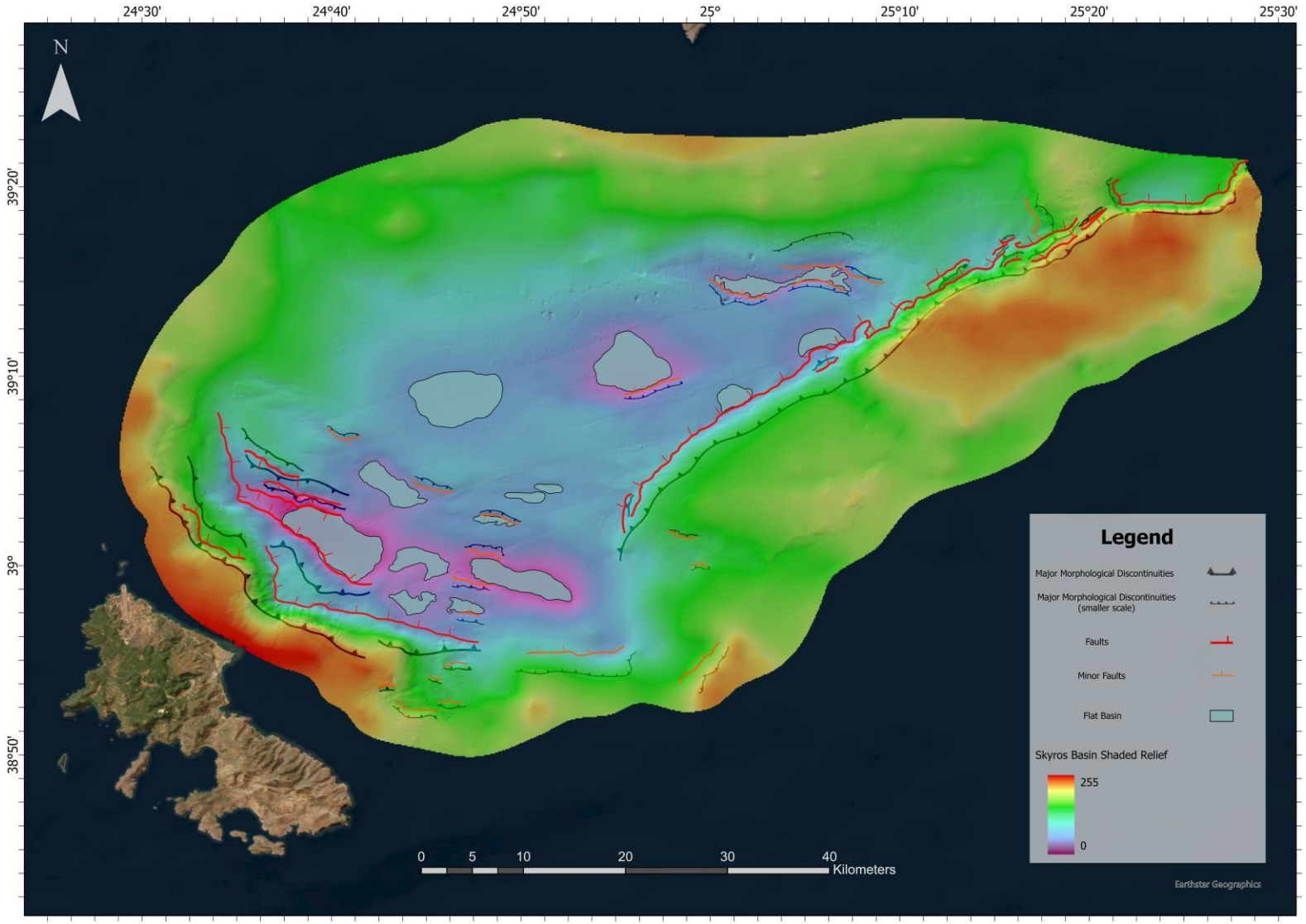

Figure 29. *Moprhotectonic Map of the Skyros basin, with faults, major morphological discontinuities, and the flat part of the basin.*

5.2. GEOMORPHOLOGICAL ANALYSIS - SYNTHETIC MAP

The synthetic map (Figure 32; Figure 33) creation tries to accomplish a geomorphological classification of the areas with features such as the continental platform, fault scarps, continental slope with <5 degrees of slope value, basinal areas, and the flat part of the basinal area. This classification can be achieved in ArcGIS using the Benthic Terrain Modeler extension with its Benthic Terrain Classification tool, and a decision table containing definitions and thresholds of only slope and depth, applied to the data to classify the aforementioned structures in the study area (Figure 30), (Figure 31). The definitions set for the geomorphological classification are after Papanikolaou et al 2002., with some small changes in depth thresholds for the Skyros area of study, because the basin is shallower. Because fault scarps are the areas delineated between the major morphological discontinuities and the minor morphological discontinuities and contain high slope values, they can be automatically depicted, but they overlap with areas of other geomorphological features.

In the NAB the fault scarps that are parallel to the Chalkidiki peninsula generally have a width of 1.5-2 kilometers, while the Fault Scarps on the SE corner of the basin to the Sithonia peninsula have a width of 4 kilometers.

In the SB the fault scarps that are parallel to Skyros's coastline generally have a width just below 2 kilometers, while the fault scarps on the eastern side of the basin are 2-2.5 kilometers.

Class	Zone	Slope_Lower	Slope_Upper	Depth_Lower	Depth_Upper
1	Continental Platform		5	-200	
2	Continental Slope <5		5	-900	-200
3	Fault Scarp	5			
4	Basinal Area	1			-900
5	Flat Basinal Area		1		-900

Figure 30. *Classification Dictionary that was used for the creation of the North Aegean Basin's Synthetic Map.*

Class	Zone	Slope_Lower	Slope_Upper	Depth_Lower	Depth_Upper
1	Continental Platform		5	-400	
2	Continental Slope <5		5	-800	-400
3	Fault Scarp	5			
4	Basinal Area	1			-800
5	Flat Basinal Area		1		-800

Figure 31. *Classification Dictionary that was used for the creation of the Skyros Basin's Synthetic Map.*

5.2.1. NORTH AEGEAN BASIN - NAB

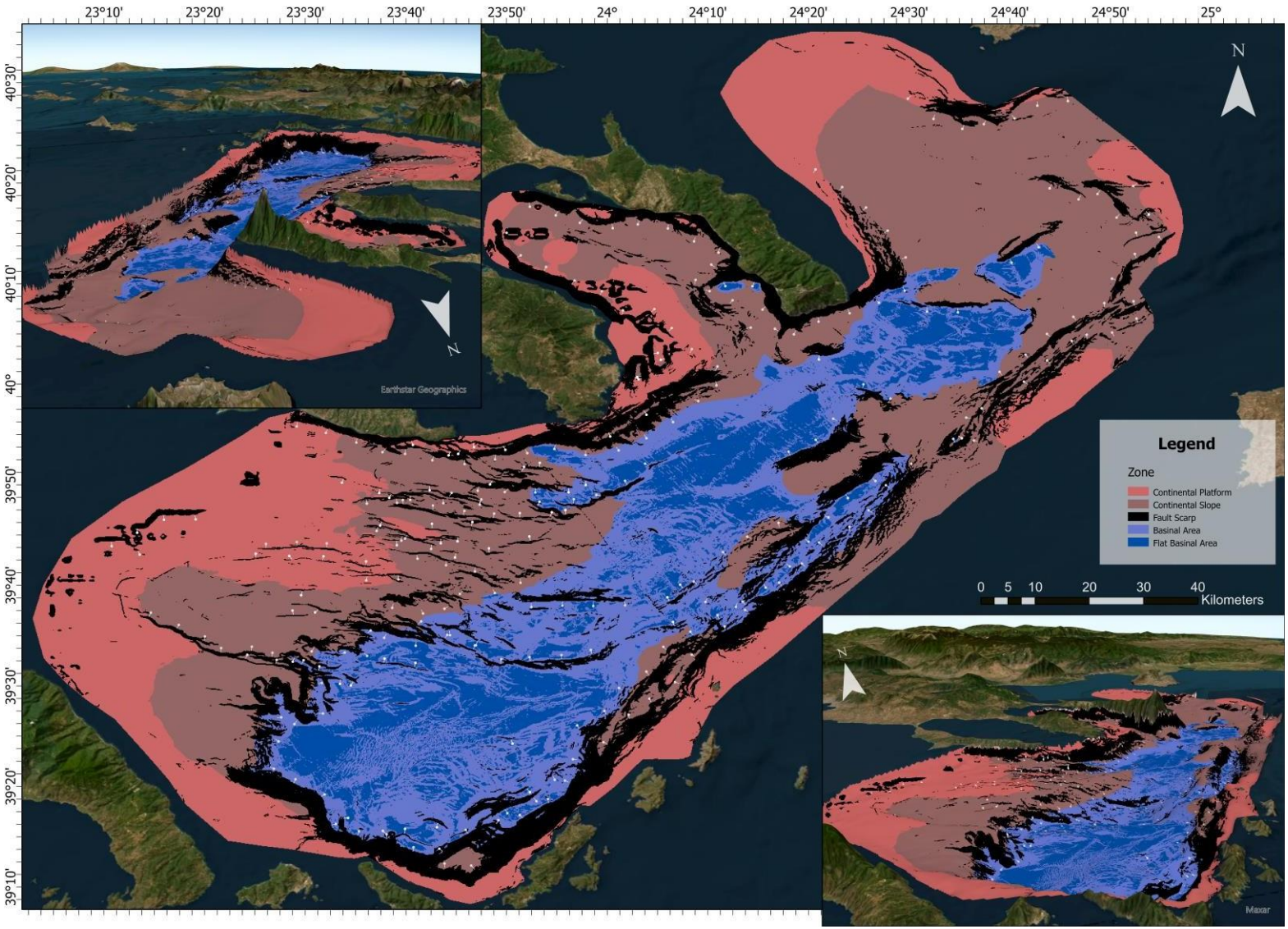

Figure 32. *Synthetic Map of the North Aegean Basin, including Landform classification with dip vectors on Fault Scarps. 3D models have a vertical exaggeration of 11.*

5.2.2. SKYROS BASIN

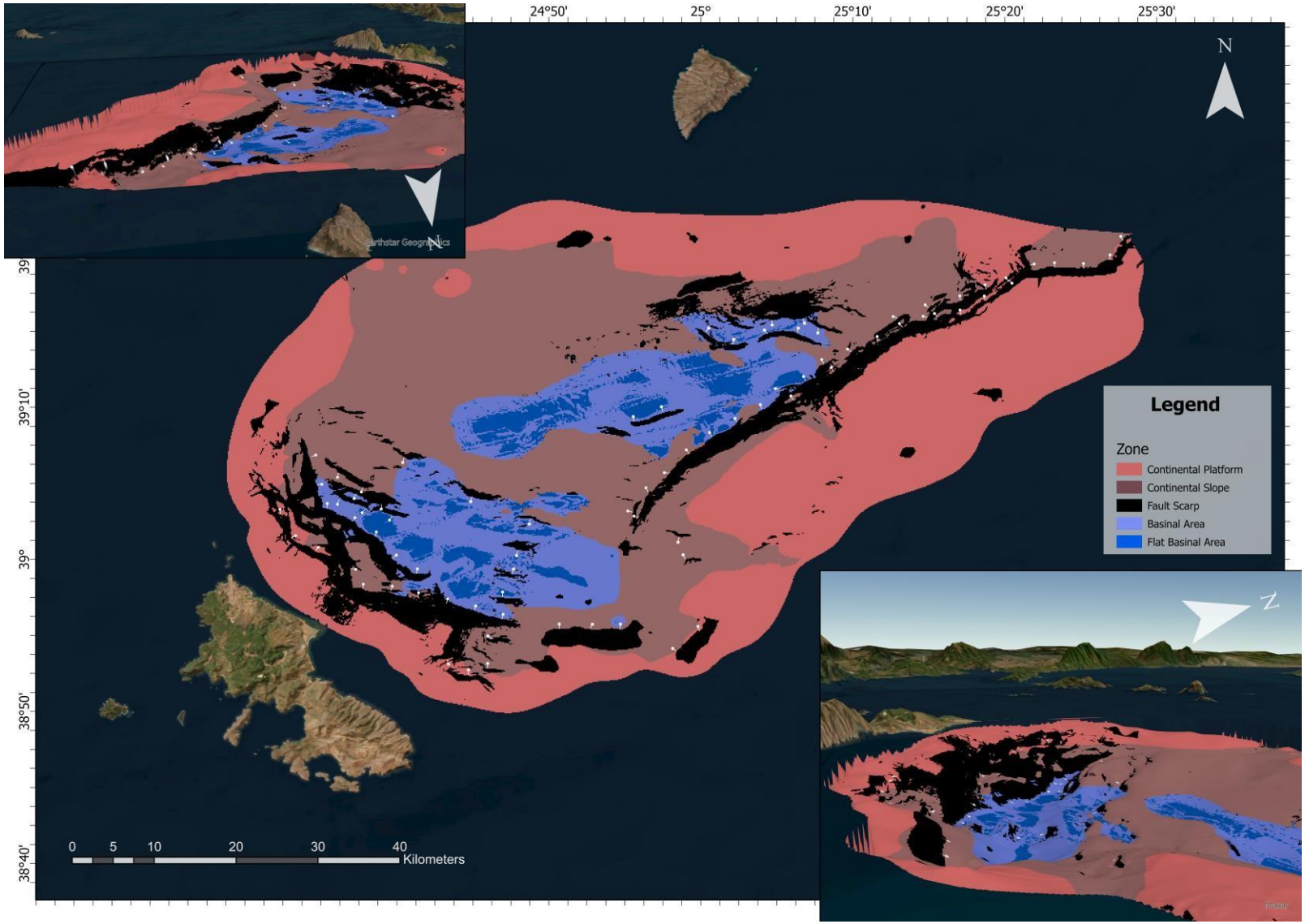

Figure 33. *Synthetic Map of the Skyros Basin, including Landform classification with dip vectors on Fault Scarps. 3D models have a vertical exaggeration of 11.*

6. DISCUSSION

From the previous analysis made it seems that Skyros Basin corresponds to the Western part of the North Aegean Sea with a NE-SW direction corresponding to the central part of the North Aegean Basin from the Chalkidiki peninsula till the NE margin. The western segment of Skyros Basin with NW-SE direction corresponds to the western margin of the NAB, comprising the outer Thermaikos Gulf down to the Northern Sporades islands until the Pelion coastline, which corresponds to the Eastern Skyros coastline. It is noteworthy that the NW-SE trending faulting component prevails in the southwestern part of both basins, whereas the NE-SW component prevails in the eastern part of both basins. According to Papanikolaou, et al., 2019, the above similarities of the two North Aegean basins imply that their triangular geometry is related to this transition from strike-slip to extension and the increasing opening and subsidence towards the SW, in agreement with the pull direction of the Hellenic subduction zone.

GPS data (McClusky, et al., 2000; Müller, et al., 2013) can be correlated to the above morphotectonic analysis of the basin, indicating an overall oblique extension towards the SW at a rate of approximately 10 mm/yr. In particular, between the GPS stations on the islands of Limnos and Skyros, McClusky, et al., 2000, calculate a motion of approximately 11 mm/yr towards the SSW, from measurements during the period 1989–1996, whereas Müller et al. (2013) extract approximately 8 mm/yr from measurements during 1993–2009. Seismotectonic data also shows the co-existence of dextral strike-slip faulting in the ENE-WSW direction as well as normal faulting with a NEW extension (Kiratzi, Wagner, & Langston, 1991; Ganas, 2005).

Regarding the seismic hazard of the NAB, the danger is high and according to Jenny et al. (2004), an M_w = 7.2–7.7 earthquake is expected every 100–500 years in the region. Furthermore, Papanikolaou (2007) estimated the maximum earthquake size of M_w = 7.1-7.6 for the southern marginal fault of the Sporades basin, depending on the rupture length. While in Skyros according to calculations (Papanikolaou, et al., 2019), the faults can yield a maximum magnitude distribution that ranges from M_w = 5.93 to M_w = 7.45. Data on focal mechanisms from 6 strong

events in the Skyros and the surrounding area indicate that 5 events (6/5/1981 Mw = 5.4, 19/2/1968 Mw = 6.8, 14/11/1997 Mw = 5.7, 19/12/1981 Mw = 6.8, 27/12/1981 Mw = 6.3) displayed predominant or pure strike-slip kinematics, whereas one event (4/3/1967 Mw = 6.2) displayed normal faulting characteristics (Kirzatzi & Louvari, 2003).

Simulations about a potential tsunami appearance in the North Aegean area during the Holocene (Alexandre, Rodriguez, Sakellarious, Lykousis, & Christian, 2019) show that the expected tsunami waves from a submarine landslide (1.85 kilometers^3 in volume based on previously recorded submarine landslides) are higher than values expected in the case of an earthquake along the North Anatolian Fault and higher than run-up values documented from tsunami deposits in the Thermaic Gulf (Reicherter, et al., 2010). However, the tsunami hazard related to submarine landslides is less severe than tsunami associated with landslides triggered during strong earthquake events (Okal, Synolakis, Uslu, Kalligeris, & Voukouvalas, 2010; Perissoratis & Papadopoulos, 1999) or tsunamis triggered during or after volcanic events (e.g. Santorini in the Bronze age (Novikova, Papadopoulos, & McCoy, 2011).

The detailed analysis of the morphological map of NAB can reveal places where such submarine landslide events have taken place, but the exact mechanism that triggered them is unknown. Specifically, three areas of landslide events were identified across the southern marginal zone of NAB (Figure 34). However, It is noteworthy that all three observed landslides occur in the tectonically active areas since they are located in the southeastern margin.

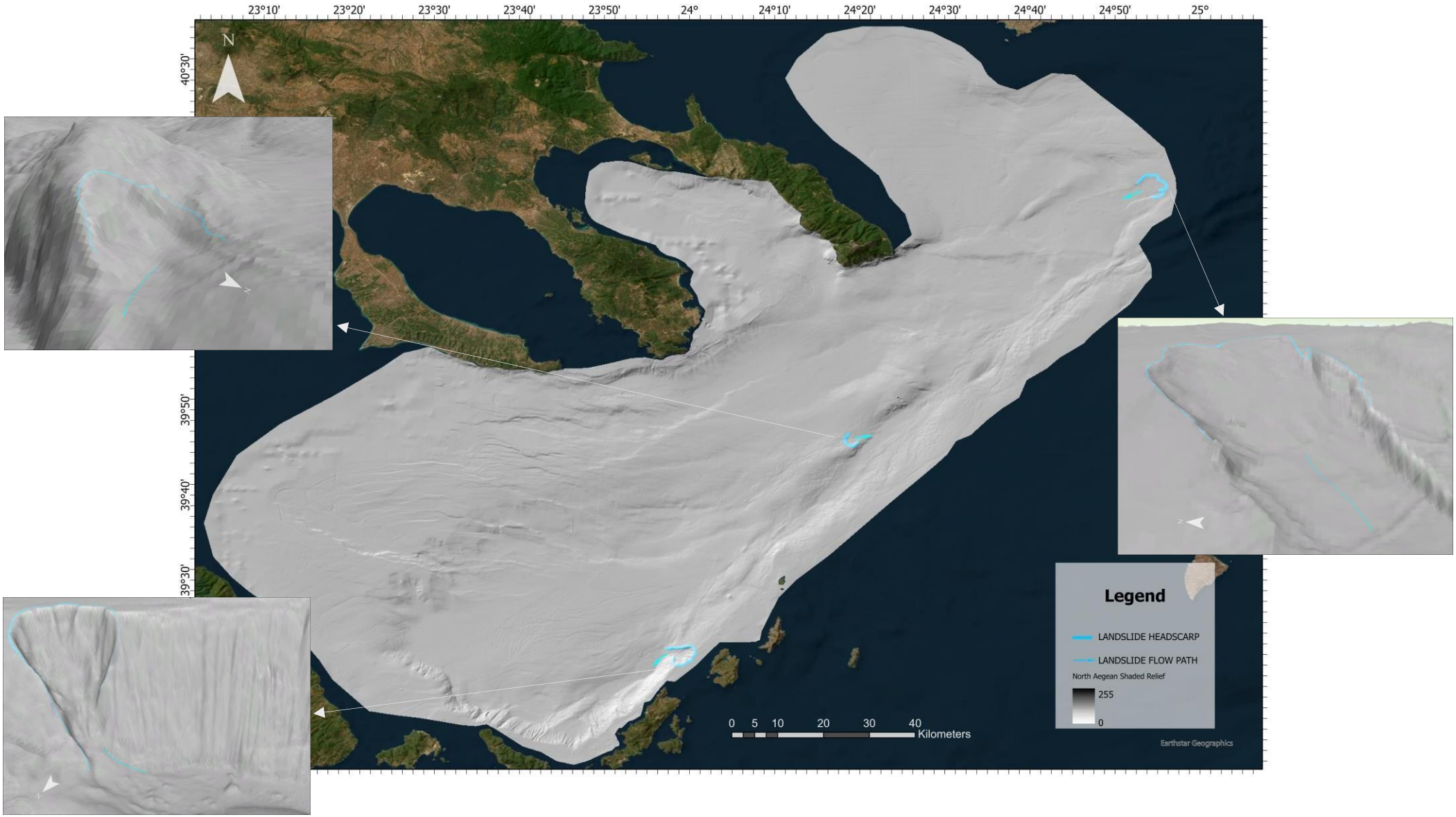

Figure 34. *Shaded Relief Map of the North Aegean Basin, including the Submarine Landslide head scarps and flow path. The previous are also depicted in 3D view, with a vertical exaggeration of 5.*

7. CONCLUSIONS

The morphotectonic analysis of the area shows that the seafloor morphology of the North Aegean is dictated by many faults, in particular by the North Anatolian Fault that created two similar structures in the area; The Skyros Basin and the North Aegean Basin. The Skyros Basin has a similar structure to the neighboring NAB but has smaller dimensions and lower deformation rates which is documented by the shallower depths (900 versus 1600 meters) and the smaller width (40 versus 20 kilometers). Both basins are characterized by NE-SW trending segmented faults that constitute the NAF in the eastern part, and NE-SW faults that dominate the western part.

Both the SB and the NAB are controlled by the NAF which is a large-scale fault and poses a highly possible future risk for seismic events that can even trigger other geological phenomena like submarine landslides and tsunamis. It is estimated that strong earthquakes exceeding $M_w >$ 6.0 (Jenny, Goes, Giardini, & Kahle, 2004) are possible in the area. The worst-case scenario implies a multi-segment rupture of the NAF both in the SB or the NAB that can produce an event of M_w > 7.0 (Papanikolaou & Royden, 2007). Such strong earthquakes can cause significantly large landslides with tsunamigenic potential that will threaten the surrounding islands and coastline.

In conclusion, higher resolution bathymetric data of the area of the NAB and the Skyros Basin would be of great importance, to map the hazardous areas and identify the susceptible areas, to prevent a catastrophic event from happening.

REFERENCES

Alexandre, J., Rodriguez, M., Sakellarious, D., Lykousis, V., & Christian, G. (2019). Tsunamigenic potential of a Holocene submarine landslide along the North Anatolian Fault (northern Aegean Sea, off Thasos island): insights from numerical modeling. *Nat. Hazards Earth Syst. Sci.*, 121-136.

Armijo, R., Meyer, B., Hubert, A., & Barka, A. (1999). Westward propagation of the North Anatolian Fault into the northern Aegean: Timing and kinematics. *Geology*, 267-270.

Armijo, R., Meyer, B., Hubert, A., & Barka, A. (1999). Westward propagation of the North Anatolian Fault into the northern Aegean: Timing and kinematics. *Geology*, 267-270.

Beniest, A., Brun, J., Gorini, C., Crombez, V., Deschamps, R., Hamon, Y., & Smit, J. (2016). Interaction between trench retreat and Anatolian escape as recorded by neogene basins in the northern Aegean Sea. *Marine and Petroleum Geology*, 30-42.

Billiris, H., Paradissis, D., Veis, G., England, P., Featherstone, W., Parsons, B., . . . Ambraseys, N. (1991). Geodetic determination of tectonic deformation in central Greece from 1900 to 1988. *Nature*, 124-129.

Brun, J., & Sokoutis, D. (2010). 45 m.y. of Aegean crust and mantle flow driven by trench retreat. *Geology*, 815-818.

Brun, J., Faccenna, C., Gueydan, F., Sokoutis, D., Philippon, M., Kydonakis, K., & Gorini, C. (2016). The two-stage Aegean extension, from localized to distributed, a result of slab rollback acceleration. *Canadian Journal of Earth Sciences*, 1142-1157.

Clarke, P., Davies, R., England, P., Parsons, B., Billiris, H., Paradissis, D., . . . Briole, P. (1998). Crustal strain in central Greece from repeated GPS measurements in the interval 1989-1997. *Geophysical Journal International*, 195-214.

Davies, R., England, P., Parsons, B., Billiris, H., Paradissis, D., & Veis, G. (1997). Geodetic strain of Greece in the interval 1892-1992. *Journal of Geophysical Research B: Solid Earth*, 24571-24588.

Dermitzakis, M., & Papanikolaou, D. (1981). Paleogeography and geodynamics of the Aegean region during the Neogene. *Annales Geologiques des Pays Helleniques*, 245–289.

Dewey, J., & Şengör, A. (1979). Aegean and surrounding regions: Complex multiplate and continuum tectonics in a convergent zone. *Bulletin of the Geological Society of America*, 84-92.

Finetti, J., Papanikolaou, D., Del Ben, A., & Karvelis, P. (1991). Preliminary geotectonic interpretation of the East Mediterranean chain and the Hellenic Arc. *Bulletin of the Geological Society of Greece*, 509-526.

Ganas, A. (2005). The 2001 Mw - 6.4 Skyros earthquake, conjugate strike-slip faulting and spatial variation in stress within the central Aegean Sea. *Geodynamics*, 61-77.

Hubert-Ferrari, A., King, G., Manighett, I., Armijo, R., Meyer, B., & Tapponnier, P. (2003). Longterm elasticity in the continental lithosphere; modelling the Aden Ridge propagation and the Anatolian extrusion process. *Geophysical Journal International*, 111-132.

Janin, A., Rodriguez, M., Sakellariou, D., Lykousis, V., & Gorini, C. (2018). Tsunamigenic potential of a Holocene submarine landslide along the North Anatolian Fault (North Aegean Sea, off Thasos Island): insights from numerical modeling. *Natural Hazards and Earth System Sciences Discussions*.

Jenny, S., Goes, S., Giardini, D., & Kahle, H. (2004). Earthquake recurrence parameters from seismic and geodetic strain rates in the Eastern Mediterranean. *Geophysical Journal International*, 1331-1347.

Kahle, H., Cocard, M., Peter, Y., Geiger, A., Reilinger, R., Barka, A., & Veis, G. (2000). GPSderived strain rate field within the boundary zones of the Eurasian, African, and Arabian plates. *Journal of Geophysical Research: Solid Earth*, 23353-23370.

Kiratzi, A., Wagner, G., & Langston, C. (1991). Source parameters of some large earthquakes in Northern Aegean determined by body waveform modeling. *Pure Appl. Geophys.*, 515-527.

Kirzatzi, A., & Louvari, E. (2003). Focal Mechanisms of shallow earthquakes in the Aegean Sea and the surrounding lands determined by body waveform modelling. *Pure Appl. Geophys.*, 251-274.

Kreemer, C., Chamot-Rooke, N., & Le Pichon, X. (2004). Constraints on the evolution and vertical coherency of deformation in the Northern Aegean from a comparison of geodetic, geologic and seismologic data. *Earth and Planetary Science Letters*, 329-346.

Kurt, H., Demirbağ, E., & Kuşçu, I. (2000). Active submarine tectonism and formation of the Gulf of Saros, Northeast Aegean Sea, inferred from multi-channel seismic reflection data. *Marine Geology*, 13-26.

Le Pichon, X., & Angelier, J. (1979). The Hellenic Arc and Trench System: A key to the neotectonic evolution of the Eastern Mediterranean Area. *Tectonophysics*, 1-42.

Le Pichon, X., & Kreemer, C. (2010). The Miocene-to-Present Kinematic Evolution of the Eastern Mediterranean and Middle East and its implications for Dynamics. *Annual Review of Earth and Planetary Sciences*, 323-351.

Le Pichon, X., Chamot-Rooke, N., Lallemant, S., Noomen, R., & Veis, G. (1995). Geodetic determination of the kinematics of central Greece with respect to Europe: Implications for eastern Mediterranean tectonics. *Journal of Geophysical Research: Solid Earth*, 12675–12690.

Le Pichon, X., Engor, A., Demirbağ, E., Rangin, C., Imren, C., Armijo, R., . . . Tok, B. (2001). The active Main Marmara Fault. *Earth and Planetary Science Letters*, 595-616.

Lister, J., Banga, G., & Feenstra, A. (1984). Metamorphic core complexes of Cordilleran type in the Cyclades, Aegean Sea, Greece. *Geology*, 221-225.

Lyberis, N. (1984). Tectonic evolution of the North Aegean Trough. In: Dixon, J.E., Robertson A.H.F. (eds), The Geological Evolution of the Eastern Mediterranean. *Geological Society, Special Publications*, 709-725.

Mascle, J., & Martin, L. (1990). Shallow structure and recent evolution of the Aegean Sea: A synthesis based on continuous reflection profiles. *Marine Geology*, 271-299.

McClusky, S., Balassanian, S., Barka, A., Demir, C., Ergintav, S., Georgiev, I., . . . Veis, G. (2000). Global Positioning System constraints on plate kinematics and dynamics in the eastern Mediterranean and Caucasus. *Journal of Geophysical Research: Solid Earth*, 5695-5719.

McKenzie, D. (1970). Plate tectonics of the mediterranean region. *Nature*, 239-243.

McNeill, L., Mille, A., Minshull, T., Bull, J., Kenyon, N., & Ivanov, M. (2004). Extension of the North Anatolian Fault into the North Aegean Trough: Evidence for transtension, strain partitioning, and analogues for Sea of Marmara basin models. *Tectonics*, 1-12.

Müller, M., Geiger, A., Kahle, H., Veis, G., Billiris, H., Paradissis, D., & Felekis, S. (2013). Velocity and deformation fields in the North Aegean domain, Greece, and implications for fault kinematics, derived from GPS data 1993-2009. *Tectonophysics*, 34-49.

Novikova, T., Papadopoulos , G., & McCoy, F. (2011). Modelling of tsunami generated by the giant late Bronze Age eruption of Thera. *Geophys. J. Int.*, 665-680.

Nyst, M., & Thatcher, W. (2004). New constraints on the active tectonic deformation of the Aegean. *Journal of Geophysical Research: Solid Earth*, 1-23.

Okal, E., Synolakis, C., Uslu, B., Kalligeris, N., & Voukouvalas, E. (2010). Aegean region and strain accumulation along the Hellenic subduction zone. *Tectonophysics*, 22-30.

Papanikolaou, D., & Royden, L. (2007). Disruption of the Hellenic arc: Late Miocene extensional detachment faults and steep Pliocene-Quaternary normal faults - Or what happened at Corinth? *Tectonics*, 1-16.

Papanikolaou, D., Alexandri, M., & Nomikou, P. (2006). Active faulting in the North Aegean Basin. *Geological Society of America Bulletin*, 189-209.

Papanikolaou, D., Alexandri, M., Nomikou, P., & Ballas, D. (2002). Morphotectonic structure of the western part of the North Aegean basin based on swath bathymetry. *Marine Geology*, 465-492.

Papanikolaou, D., Nomikou, P., Papanikolaou, I., Lampridou, D., Rousakis, G., & Alexandr, M. (2019). Active tectonics and seismic hazard in Skyros Basin, North Aegean Sea. *Marine Geology*, 94-110.

Perissoratis, C., & Papadopoulos, G. (1999). Sediment instability and slumping in the southern Aegean Sea and the case history of the 1956 tsunami. *Marine Geology*, 287-305.

Pérouse, E., Chamot-Rooke, N., Rabaute, A., Briole, P., Jouanne, F., Georgiev, I., & Dimitrov, D. (2012). Bridging onshore and offshore present-day kinematics of central and eastern Mediterranean: Implications for crustal dynamics and mantle flow. *Geochemistry, Geophysics, Geosystems*, 1-25.

Philippon, M., Brun, J., Gueydan, F., & Sokoutis, D. (2014). The interaction between Aegean back-arc extension and Anatolia escape since Middle Miocene. *Tectonophysics*, 176-188.

Reicherter, K., Papanikolaou, I., Roger, J., Mathes-Schmidt, M., Papanikolaou, D., Rössler, S., . . . Stamatis, G. (2010). Holocene tsunamigenic sediments and tsunami modelling in the Thermaikos Gulf area (northern Greece). *Z. Geomorphol. Supp.*, 99-125.

Reilinger, R., McClusky, S., Vernant, P., Lawrence, S., Ergintav, S., Cakmak, R., . . . Karam, G. (2006). GPS constraints on continental deformation in the Africa-Arabia-Eurasia continental collision zone and implications for the dynamics of plate interactions. *Journal of Geophysical Research*, 1-26.

Roussos, N., & Lyssimachou, T. (1991). Structure of the central north aegean trough: An active strike-slip deformation zone. *Basin Research*, 37-46.

Sakellariou, D., Drakopoulou, V., Rousakis, G., Livanos, I., Loukaidi, V., Kyriakidou, C., . . . Manta, K. (2022). Geomorphological Features. 20-119.

Sakellariou, D., Mascle, J., & Lykousis, V. (2013). Strike slip tectonics and transtensional deformation in the Aegean region and the Hellenic arc: Preliminary results. *Bulletin of the Geological Society of Greece*, 647-656.

Sakellariou, D., Rousakis, G., Morfis, I., Panagiotopoulos, I., Ioakim, C., Trikalinou, G., . . . Karageorgis, A. (2018). Deformation and kinematics at the termination of the North Anatolian Fault: the North Aegean Trough. *INQUA Focus Group Earthquake Geology and Seismic Hazards*, 237-240.

Şengör, A., Tüysüz, O., Imren, C., Sakinç, M., Eyidoğan, H., Görür, N., . . . Rangin, C. (2005). The North Anatolian Fault: A new look. *Annual Review of Earth and Planetary Sciences*, 37-112.